Computer Assisted Mechanics and Engineering Sciences, 5: 201–226, 1998.

Symmetric boundary element method for "discrete" crack modelling of fracture processes

Giulio Maier and Attilio Frangi
Department of Structural Engineering, Technical University (Politecnico) of Milan, Piaza Leonardo da Vinci 32, Milan 20133, Italy

(Received November 3, 1997)

Dedicated to Professor Zdenek Bazănt, on the occasion of his 60th anniversary

Analysis of fracture processes in structures of quasi-brittle concrete-like materials is here discussed on the basis of discrete cohesive crack models and of a nontraditional boundary element method. This method, called "symmetric Galerkin BEM", is characterized by the combined use of static and kinematic sources (i.e. traction and displacement discontinuities) to generate a symmetric integral operator by its space-discretization in the Galerkin weighted-residual sense. Consistently, the discrete crack model is enforced in a weak sense and expressed in terms of Prager's generalized variables. On this basis, some of the main aspects of a computational theory of quasi-brittle fracture mechanics are presented and discussed.

1. Introduction

This paper is intended to present a conspectus of a recently developed boundary element method (BEM), named symmetric Galerkin method (SGBEM) in view of its use in nonlinear fracture mechanics of concrete structures. Several models have been proposed in the literature for the simulation, to engineering purposes, of fracture processes in concrete and other quasi-brittle ("disordered") materials. The kind of fracture idealization assumed herein, and discussed only as for its analytical description, is the discrete cohesive crack model (CCM) stemming from classical works of Barenblatt (1962), Dugdale, Hillerborg and others.

This model relegates all nonlinearity to a discontinuity locus, say Γ_d, the dimensionality of which is smaller by one with respect to that of the domain over which the analysis is formulated. The consequent presence of a dominant linear-elastic background in fracture simulation problems based on the CCM, tends to privilege BEMs over finite element methods (FEMs) and, in particular, the SGBEM among BEMs, mainly because of the reasons pointed out below. The following symbols are adopted henceforth (boldfaces for matrices and vectors): $\mathbf{x}$, $\boldsymbol{\xi}$ = Cartesian coordinates; Γ_d = locus of (actual or potential) displacement discontinuities; $\mathbf{w}$, $\mathbf{p}$ = displacement jumps and tractions across Γ_d; $\mathbf{p}^E$, $\mathbf{Z}(\mathbf{x}, \boldsymbol{\xi})$ = tractions due to the given external actions and matrix of influence (Green's) functions of $\mathbf{p}$ due to $\mathbf{w}$, respectively, in a purely linear elastic situation (i.e. in the absence of any kinematic discontinuity).

With this symbology, the nonlinear response to external actions of the structure, idealized according to the CCM, can be conceived as governed by the following relationships:

$$\mathbf{p}(\mathbf{x}, t) = f[\mathbf{w}(\mathbf{x}, \tau; 0 \leq \tau \leq t)] \quad \mathbf{x} \in \Gamma_d \,, \tag{1}$$

$$\mathbf{p}(\mathbf{x}, t) = \int_{\Gamma_d} \mathbf{Z}(\mathbf{x}, \boldsymbol{\xi}) \mathbf{w}(\boldsymbol{\xi}, t) \mathrm{d}\Gamma_{\boldsymbol{\xi}} + \mathbf{p}^E(\mathbf{x}, t) \quad \mathbf{x} \in \Gamma_d \,. \tag{2}$$

Equation (1) symbolically formulates the analytical description of the adopted CCM, generally history-dependent, t and τ being time instants, see Sec. 5; Eq.(2) concisely captures geometry and elasticity of the structure in point, and expresses superposition of effects, thus exploiting at most the background linearity of the problem.

Clearly, whenever the unknown field $\mathbf{w}$ is computed by solving Eqs. (1) and (2), any other quantity of interest, in any other point of the domain Ω occupied by the structure, can be evaluated by customary linear computations, not of concern here.

It is worth noting that, if Ω were to coincide with the two- or three dimensional space Ω_∞, then $\mathbf{Z}$ would acquire simple analytical expressions (later referred to by symbol $\mathbf{G}_{pp}$) emerged from the mathematical theory of elasticity in the last century. In practical situations $\mathbf{Z}$ is not known and an approximation of it is required for engineering applications of the above formulation of fracture analysis, i.e. the integral equation (2) must be suitably approximated by a linear algebraic equation. To this purpose the SGBEM appears to be ideally suited for the following three main reasons.

(a) The SGBEM involves only variables on the boundary Γ and on the locus Γ_d. The former variables can be condensed economically by inverting a symmetric matrix of coefficients, while any FEM would involve domain variables as well and in traditional BEMs the matrix to invert is non-symmetric.

(b) Unlike traditional (collocation) BEMs, the resulting discrete influence operator, say $\tilde{\mathbf{Z}}$, preserves the essential properties of the kernel $\mathbf{Z}$ in Eq. (2). These properties are: symmetry in the sense that $\mathbf{Z}(\mathbf{x}, \boldsymbol{\xi}) = \mathbf{Z}^T(\boldsymbol{\xi}, \mathbf{x})$, $\mathbf{x} \neq \boldsymbol{\xi}$, as it can be shown on the basis of Betti theorem of linear elasticity; negative definiteness of the associated quadratic form which has the meaning of the opposite of the elastic strain energy due to the distorsions $\mathbf{w}$ imposed on Γ_d. The discretization according to the SGBEM leads to a structural model with the mechanical features of the original continuum and, hence, susceptible of a complete mechanical theory of remarkable computational interest.

(c) The SGBEM exhibits superior accuracy and convergence properties with respect to traditional BEMs, as it is now widely recognized, whereas the significant mathematical and numerical difficulties related to the hypersingular integrations nowadays can be regarded as largely overcome.

The above points are substantiated in a growing literature on SGBEM in general, see e.g. [4, 14, 28, 36, 47, 49, 50, 51, 56, 57, 61], and on its fracture mechanics applications, see e.g. [9, 48, 50, 52]. Some fundamentals of the SGBEM are covered by recent books on BEMs [3, 15, 37]; traditional (nonsymmetric) BEMs applied to linear elastic fracture mechanics are comprehensively expounded e.g. in [24, 25].

The present survey of recent and current developments in the title subject covers the following topics: the generation of the integral equations (Sec. 2); their space discretization by a weak weighted residual approach, to fracture analysis purposes (Sec. 3); a general procedure to compute the double hypersingular integrals involved in the generation of the coefficient matrix (Sec. 4); analytical descriptions of history-dependent (nonholonomic) CCMs (Sec. 5); special classes of holonomic CCM (Sec. 10); a weak formulation of CCM in generalized variables (Sec. 7); overall stability and bifurcation criteria emerging from the rate formulation (Sec. 8); time-stepping solution procedures (Sec. 9); history-independent (holonomic) analysis, multiplicity of solutions and numerical algorithms (Sec. 10).

2. Generation of a Symmetric Boundary Integral Operator

Consider a two-dimensional (2D) or three dimensional (3D) elastic space Ω_∞ subject to external forces $\mathbf{f}^*$ (statical or "single layer" or "stress discontinuity" sources) and imposed displacement discontinuities $\mathbf{d}^*$ (kinematic or "double layer" sources or distorsions) distributed over its locus Γ^* (a line in 2D, surface in 3D).

Displacements $\mathbf{u}^*$ and tractions $\mathbf{p}^*$ due to these external actions can be expressed by superposition of effects (for $\mathbf{x}$ not on Γ^*) as follows:

$$\mathbf{u}^*(\mathbf{x}) = \int_{\Gamma^*} \mathbf{G}_{uu}(\mathbf{x},\boldsymbol{\xi})\mathbf{f}^*(\boldsymbol{\xi})\mathrm{d}\Gamma_\xi + \int_{\Gamma^*} \mathbf{G}_{up}(\mathbf{x},\boldsymbol{\xi})\mathbf{d}^*(\boldsymbol{\xi})\mathrm{d}\Gamma_\xi \,, \tag{3}$$

$$\mathbf{p}^*(\mathbf{x}) = \int_{\Gamma^*} \mathbf{G}_{pu}(\mathbf{x},\boldsymbol{\xi})\mathbf{f}^*(\boldsymbol{\xi})\mathrm{d}\Gamma_\xi + \int_{\Gamma^*} \mathbf{G}_{pp}(\mathbf{x},\boldsymbol{\xi})\mathbf{d}^*(\boldsymbol{\xi})\mathrm{d}\Gamma_\xi. \tag{4}$$

Matrices $\mathbf{G}_{hk}$ contain Green's influence functions for Ω_∞, once for all expressed by simple classical formulae (simple for isotropic materials) available in textbooks, e.g. [15, 37]. Specifically: for $k = u$ Kelvin (1848) fundamental solution; for $k = p$ influence functions for the effects of distorsions (Gebbia's kernel). Crucial mathematical features of these functions and their integrals will be briefly discussed in Sec. 4.

Consider now the real structure contained in the domain $\bar{\Omega} = \Omega \cup \Gamma$ of Ω_∞. Its boundary Γ consists of two disjoint complementary parts Γ_p and Γ_u subjected to given forces $\bar{\mathbf{p}}$ and displacements $\bar{\mathbf{u}}$, respectively (external actions in Ω are assumed zero for brevity). A frequently adopted starting point of BEMs in elasticity is Betti's identity involving the real elastic state (unstarred symbols) and a fictitious one (starred symbols), the integration coordinate $\mathbf{x}$ being interpreted as running on the "internal face" Γ^- of Γ (i.e. $\mathbf{x} \equiv \mathbf{x}^- \in \Gamma^-$, with Γ^- denoting a set of points of Ω infinitely close to Γ). Here the locus Γ_d of possible kinematic discontinuities must be allowed for in Betti's identity, which reads

$$\int_\Gamma \mathbf{p}^T\mathbf{u}^*\mathrm{d}\Gamma_x - \int_{\Gamma_d} \mathbf{p}^T\mathbf{w}^*\mathrm{d}\Gamma_x = \int_\Gamma \mathbf{u}^T\mathbf{p}^*\mathrm{d}\Gamma_x - \int_{\Gamma_d} \mathbf{w}^T\mathbf{p}^*\mathrm{d}\Gamma_x. \tag{5}$$

A usual path starts leading to conventional BEMs, see e.g. [3, 15, 37], when the fictitious elastic state is identified with Kelvin's fundamental solutions: these are contained in function matrices $\mathbf{G}_{uu}$ and $\mathbf{G}_{pu}$, each column of which represents effects in Ω_∞ due to a unit force acting in $\boldsymbol{\xi}$ in the direction of the relevant coordinate axis. Thus Eq. (5) gives rise to a classical Somigliana integral equation.

Instead of the above traditional path, an itinerary leading to the SGBEM of concern here may be initiated by choosing static sources $\mathbf{f}^*$ acting on the constrained boundary Γ_u, and kinematic sources $\mathbf{d}^*$ on both the unconstrained boundary Γ_p (denoted by $\widehat{\mathbf{d}}^*$) and the discontinuity locus Γ_d (denoted by $\mathbf{w}^*$). It is worth stressing that the real structure $\bar{\Omega}$ ($\bar{\Omega} = \Omega \cup \Gamma$) is conceived as embedded in Ω_∞ when writing Eqs. (3) and (4) for $\mathbf{x} \in \Omega$, so that in Eq. (5) we have: $\Gamma^* = \Gamma \cup \Gamma_d = \Gamma_u \cup \Gamma_p \cup \Gamma_d$.

Let now Eqs. (3) and (4), specialized by means of the above provisions, be substituted into Betti's equation (5). Thus (argument $(\mathbf{x}, \boldsymbol{\xi})$ of kernels being omitted for brevity), Eq. (5) becomes:

$$\begin{aligned}
0 = &\int_{\Gamma_u} \mathbf{f}^{*T}(\boldsymbol{\xi}) \left\{ \int_\Gamma \left[\mathbf{G}_{uu}^T\mathbf{p}(\mathbf{x}) - \mathbf{G}_{pu}^T\mathbf{u}(\mathbf{x})\right] \mathrm{d}\Gamma_x + \int_{\Gamma_d} \mathbf{G}_{pu}^T\mathbf{w}(\mathbf{x})\mathrm{d}\Gamma_x \right\} \mathrm{d}\Gamma_\xi \\
&+ \int_{\Gamma_p} \widehat{\mathbf{d}}^{*T}(\boldsymbol{\xi}) \left\{ \int_\Gamma \left[\mathbf{G}_{up}^T\mathbf{p}(\mathbf{x}) - \mathbf{G}_{pp}^T\mathbf{u}(\mathbf{x})\right] \mathrm{d}\Gamma_x + \int_{\Gamma_d} \mathbf{G}_{pp}^T\mathbf{w}(\mathbf{x})\mathrm{d}\Gamma_x \right\} \mathrm{d}\Gamma_\xi \\
&+ \int_{\Gamma_d} \mathbf{w}^{*T}(\boldsymbol{\xi}) \left\{ \int_\Gamma \left[\mathbf{G}_{up}^T\mathbf{p}(\mathbf{x}) - \mathbf{G}_{pp}^T\mathbf{u}(\mathbf{x})\right] \mathrm{d}\Gamma_x + \int_{\Gamma_d} \mathbf{G}_{pp}^T\mathbf{w}(\mathbf{x})\mathrm{d}\Gamma_x - \mathbf{p}(\boldsymbol{\xi}) \right\} \mathrm{d}\Gamma_\xi \,.
\end{aligned} \tag{6}$$

Since Eq. (6) holds for any arbitrarily chosen source densities $\mathbf{f}^*$, $\widehat{\mathbf{d}}^*$ and $\mathbf{w}^*$, the expressions in parentheses $\{\}$ must vanish individually and, therefore, they give rise to three integral equations.

These generate the following three boundary integral equations (BIEs), when the data $\bar{\mathbf{p}}$ on Γ_p^- and $\bar{\mathbf{u}}$ on Γ_u^-, are entered in them, while $\mathbf{p}$ for $\mathbf{x} \in \Gamma_u^-$, $\mathbf{u}$ on Γ_p^- and $\mathbf{w}$ on Γ_d are recognized as unknowns in the actual problem:

$$\int_{\Gamma_u} \mathbf{G}_{uu}^T \mathbf{p}(\mathbf{x}) d\Gamma_x - \int_{\Gamma_p} \mathbf{G}_{pu}^T \mathbf{u}(\mathbf{x}) d\Gamma_x + \int_{\Gamma_d} \mathbf{G}_{pu}^T \mathbf{w}(\mathbf{x}) d\Gamma_x = \bar{\mathbf{g}}_u(\boldsymbol{\xi}), \qquad \boldsymbol{\xi} \in \Gamma_u, \tag{7}$$

$$-\int_{\Gamma_u} \mathbf{G}_{up}^T \mathbf{p}(\mathbf{x}) d\Gamma_x + \int_{\Gamma_p} \mathbf{G}_{pp}^T \mathbf{u}(\mathbf{x}) d\Gamma_x - \int_{\Gamma_d} \mathbf{G}_{pp}^T \mathbf{w}(\mathbf{x}) d\Gamma_x = \bar{\mathbf{g}}_p(\boldsymbol{\xi}), \qquad \boldsymbol{\xi} \in \Gamma_p, \tag{8}$$

$$\int_{\Gamma u} \mathbf{G}_{up}^T \mathbf{p}(\mathbf{x}) d\Gamma_x - \int_{\Gamma_p} \mathbf{G}_{pp}^T \mathbf{u}(\mathbf{x}) d\Gamma_x + \int_{\Gamma d} \mathbf{G}_{pp}^T \mathbf{w}(\mathbf{x}) d\Gamma_x = \bar{\mathbf{g}}_p(\boldsymbol{\xi}) + \mathbf{p}(\boldsymbol{\xi}), \qquad \boldsymbol{\xi} \in \Gamma_d. \tag{9}$$

The vector-valued functions $\bar{\mathbf{g}}$ on the r.h.s. of Eqs. (7)–(9) gather all data (boundary data $\bar{\mathbf{p}}$, $\bar{\mathbf{u}}$ and possible domain data, such as body forces and thermal strains, here ignored for brevity).

Betti theorem, Eq. (5), if suitably specialized and applied to Ω_∞, induces in the influence (Green's) kernels $\mathbf{G}$ a reciprocity relationship with far-reaching consequences:

$$\mathbf{G}_{hk}^T(\mathbf{x}, \boldsymbol{\xi}) = \mathbf{G}_{kh}(\boldsymbol{\xi}, \mathbf{x}), \qquad \mathbf{x} \neq \boldsymbol{\xi}, \qquad h, k = u, p. \tag{10}$$

As a first consequence, it can be shown that [61], if all integrals on the l.h.s. of Eqs. (7)–(9) are gathered in a single (linear, integral) operator, say $\mathbf{L}$, which operates on the unknown boundary fields, say $\mathbf{y} \equiv \{\mathbf{p}^T, \mathbf{u}^T, \mathbf{w}^T\}^T$, this operator is "symmetric" (or self-adjoint) in the sense that, denoting by $<,>$ the bilinear form associated to it and by $\forall$ the expression "for any", we can write:

$$< \mathbf{y}', \mathbf{L}\mathbf{y}'' > = < \mathbf{y}'', \mathbf{L}\mathbf{y}' >, \quad \forall \mathbf{y}', \mathbf{y}''. \tag{11}$$

Suppose that tractions $\mathbf{p}$ in Eq. (9) are given along the discontinuity locus Γ_d (as, e.g., Γ_d were a pressurized nonpropagating noncohesive crack). Then the solution $\mathbf{y}$ to the above BIEs would be characterized by a variational (saddle point) property, straightforwardly derivable from Eq. (11), see e.g. [61].

Suppose now that $\mathbf{w}$ is known, namely that it represents displacement discontinuities (or "distorsions") imposed along Γ_d by an external agency. Then Eqs.(7) and (8) are BIEs governing the boundary unknowns $\mathbf{p}$, $\mathbf{u}$; their unique solution is characterized by the above variational theorem concerning an integral operator $\mathbf{L}$ reduced accordingly. Then Eq. (9) is decoupled from Eqs. (7) and (8), and can be subsequently used to compute the tractions $\mathbf{p}$ across Γ_d on the basis of the boundary solution.

It is worth noting that in traditional BEMs the above symmetries and variational properties are missing. However, the above formulation of symmetric BIEs has deliberately ignored the peculiar difficulties arising from the "hypersingular" nature of kernel $\mathbf{G}_{pp}$, absent in BEMs. This issue, satisfactorily understood and resolved only in the last few years, will be discussed in Sec. 4, since it is crucial for both the mathematical rigour and the computational efficiency of the SGBEM adopted herein.

3. Space discretization of the integral equations

Following well-established procedures, the boundary Γ and the discontinuity locus Γ_d are now discretized into boundary elements (BEs). Denoting by $\mathcal{M}$ the "master element" (e.g.: the unit square $\{0 \leq \eta_1 \leq 1, 0 \leq \eta_2 \leq 1\}$ or the triangle $\{0 \leq \eta_1 \leq 1, 0 \leq \eta_2 \leq \eta_1\}$ in 3D; the unit segment $0 \leq \eta \leq 1$ in 2D), it is assumed that each boundary element, as an approximation of a portion of Γ or Γ_d, is mapped onto $\mathcal{M}$ by means of a non-singular, one-to-one transformation $x_i = x_i(\eta_1, \eta_2)$

in 3D and $x_i = x_i(\eta)$ in 2D, containing as parameters the Cartesian coordinates of suitably chosen nodes on the BE.

On each BE, tractions, displacements or displacement discontinuities are interpolated from nodal values using polynomial shape functions, as customary also in other discretization techniques like finite element methods (FEMs). By defining each shape function pertaining to a node over the whole locus where the relevant variable is defined (not only over the BE or over the "support" of that node) and by collecting all the local nodal values in vectors $\mathbf{P}_\Gamma$, $\mathbf{U}_\Gamma$ and $\mathbf{W}$, the global representations of the modelled unknown fields $\mathbf{p}$, $\mathbf{u}$ and $\mathbf{w}$ are, respectively:

$$\mathbf{p}(\mathbf{x}) = \boldsymbol{\Psi}_p(\mathbf{x})\mathbf{P}_\Gamma, \quad \mathbf{x} \in \Gamma_u; \quad \mathbf{u}(\mathbf{x}) = \boldsymbol{\Psi}_u(\mathbf{x})\mathbf{U}_\Gamma, \quad \mathbf{x} \in \Gamma_p; \quad \mathbf{w}(\mathbf{x}) = \boldsymbol{\Psi}_w(\mathbf{x})\mathbf{W}, \quad \mathbf{x} \in \Gamma_d. \tag{12}$$

It is worth noting that the assemblage of all local nodal values is implicit in Eq. (12). Continuity C^0 has been assumed for $\mathbf{u}$ on Γ and for $\mathbf{w}$ on Γ_d, for reasons clarified later in Sec. 4.

The discretized equations of the SGBEM are then obtained by enforcing Eqs. (7)–(9) in a Galerkin weighted-residuals fashion, i.e. by weighting them with the same shape functions adopted for the modelling of $\mathbf{u}$, $\mathbf{p}$ and $\mathbf{w}$, specifically with: $\boldsymbol{\Psi}_p^T(\boldsymbol{\xi})$, $\boldsymbol{\xi} \in \Gamma_u$, for Eq. (7); $\boldsymbol{\Psi}_u^T(\boldsymbol{\xi})$, $\boldsymbol{\xi} \in \Gamma_p$, for Eq. (8); $\boldsymbol{\Psi}_w^T(\boldsymbol{\xi})$, $\boldsymbol{\xi} \in \Gamma_d$, for Eq. (9). Thus, the discretized version of Eqs. (7)–(9) reads:

$$\left(\int_{\Gamma_u}\int_{\Gamma_u} \boldsymbol{\Psi}_p^T(\boldsymbol{\xi})\mathbf{G}_{uu}^T\boldsymbol{\Psi}_p(\mathbf{x})\mathrm{d}\Gamma_x\mathrm{d}\Gamma_\xi \right)\mathbf{P}_\Gamma - \left(\int_{\Gamma_u}\int_{\Gamma_p} \boldsymbol{\Psi}_p^T(\boldsymbol{\xi})\mathbf{G}_{pu}^T\boldsymbol{\Psi}_u(\mathbf{x})\mathrm{d}\Gamma_x\mathrm{d}\Gamma_\xi \right)\mathbf{U}_\Gamma$$
$$+ \left(\int_{\Gamma_u}\int_{\Gamma_d} \boldsymbol{\Psi}_p^T(\boldsymbol{\xi})\mathbf{G}_{pu}^T\boldsymbol{\Psi}_w(\mathbf{x})\mathrm{d}\Gamma_x\mathrm{d}\Gamma_\xi \right)\mathbf{W} = \int_{\Gamma_u} \boldsymbol{\Psi}_p^T(\boldsymbol{\xi})\bar{\mathbf{g}}_u(\boldsymbol{\xi})\mathrm{d}\Gamma_\xi, \tag{13}$$

$$- \left(\int_{\Gamma_p}\int_{\Gamma_u} \boldsymbol{\Psi}_u^T(\boldsymbol{\xi})\mathbf{G}_{up}^T\boldsymbol{\Psi}_p(\mathbf{x})\mathrm{d}\Gamma_x\mathrm{d}\Gamma_\xi \right)\mathbf{P}_\Gamma + \left(\int_{\Gamma_p}\int_{\Gamma_p} \boldsymbol{\Psi}_u^T(\boldsymbol{\xi})\mathbf{G}_{pp}^T\boldsymbol{\Psi}_u(\mathbf{x})\mathrm{d}\Gamma_x\mathrm{d}\Gamma_\xi \right)\mathbf{U}_\Gamma$$
$$- \left(\int_{\Gamma_p}\int_{\Gamma_d} \boldsymbol{\Psi}_u^T(\boldsymbol{\xi})\mathbf{G}_{pp}^T\boldsymbol{\Psi}_w(\mathbf{x})\mathrm{d}\Gamma_x\mathrm{d}\Gamma_\xi \right)\mathbf{W} = \int_{\Gamma_p} \boldsymbol{\Psi}_u^T(\boldsymbol{\xi})\bar{\mathbf{g}}_p(\boldsymbol{\xi})\mathrm{d}\Gamma_\xi, \tag{14}$$

$$\left(\int_{\Gamma_d}\int_{\Gamma_u} \boldsymbol{\Psi}_w^T(\boldsymbol{\xi})\mathbf{G}_{up}^T\boldsymbol{\Psi}_p(\mathbf{x})\mathrm{d}\Gamma_x\mathrm{d}\Gamma_\xi \right)\mathbf{P}_\Gamma - \left(\int_{\Gamma_d}\int_{\Gamma_p} \boldsymbol{\Psi}_w^T(\boldsymbol{\xi})\mathbf{G}_{pp}^T\boldsymbol{\Psi}_u(\mathbf{x})\mathrm{d}\Gamma_x\mathrm{d}\Gamma_\xi \right)\mathbf{U}_\Gamma$$
$$+ \left(\int_{\Gamma_d}\int_{\Gamma_d} \boldsymbol{\Psi}_w^T(\boldsymbol{\xi})\mathbf{G}_{pp}^T\boldsymbol{\Psi}_w(\mathbf{x})\mathrm{d}\Gamma_x\mathrm{d}\Gamma_\xi \right)\mathbf{W} = \int_{\Gamma_d} \boldsymbol{\Psi}_w^T(\boldsymbol{\xi})\left[\bar{\mathbf{g}}_d(\boldsymbol{\xi}) + \mathbf{p}(\boldsymbol{\xi})\right]\mathrm{d}\Gamma_\xi. \tag{15}$$

The evaluation of the double integrals in Eqs. (13)–(15) finally leads to an algebraic linear system endowed with a symmetric matrix, as it can be verified by careful inspection of Eqs. (13)–(15), taking into account the kernel reciprocity relations Eq. (10). In view of the integrations to perform, some special aspects arise, not considered here, in the transition from zones where unknown displacements are modelled (Γ_p) to those where tractions and displacements discontinuities are (Γ_u, Γ_d). These details can be found in [49, 61]. Through self-evident definitions of the new symbols (with superscripts) the algebraic system Eqs. (13)–(15) after the integrations can be re-cast in the form:

$$\begin{bmatrix} \mathbf{G}_{uu}^{uu} & -\mathbf{G}_{pu}^{pu} & \mathbf{G}_{pu}^{du} \\ -\mathbf{G}_{up}^{up} & \mathbf{G}_{pp}^{pp} & -\mathbf{G}_{pp}^{dp} \\ \mathbf{G}_{up}^{ud} & -\mathbf{G}_{pp}^{pd} & \mathbf{G}_{pp}^{dd} \end{bmatrix} \begin{Bmatrix} \mathbf{P}_\Gamma \\ \mathbf{U}_\Gamma \\ \mathbf{W} \end{Bmatrix} = \begin{Bmatrix} \bar{\mathbf{G}}^u \\ \bar{\mathbf{G}}^p \\ \bar{\mathbf{G}}^d + \mathbf{P} \end{Bmatrix}, \tag{16}$$

where the upper indices in the system matrix refer to the boundary zones where actual variables (**u**, **p**, **w**) and test functions must be integrated. In fact, if triplets $\{r,h',h\}$ and $\{s,k',k\}$ are allowed to assume any of (and only) the values $\{u,p,u\}$, $\{p,u,p\}$, $\{d,w,p\}$, the double integrals in Eqs. (13)–(15) can be covered by the following unified expression which specifies the meaning of all submatrices of coefficients in Eq. (16):

$$\mathbf{G}^{rs}_{hk} \equiv \int_{\Gamma_s}\int_{\Gamma_r} \mathbf{\Psi}^T_{k'}(\boldsymbol{\xi})\mathbf{G}^T_{hk}\mathbf{\Psi}_{h'}(\mathbf{x})\mathrm{d}\Gamma_x\mathrm{d}\Gamma_\xi. \tag{17}$$

In Eq. (16) **P** are weighted averages of tractions or "generalized tractions" on Γ_d.

The $\tilde{\mathbf{Z}}$ matrix mentioned in Sec. 1, which is intended to be a discrete approximation of the $\mathbf{Z}(\mathbf{x},\boldsymbol{\xi})$ matrix of functions in Eq. (2), can be obtained from Eq. (16) by condensation of the $\mathbf{U}_\Gamma$, $\mathbf{P}_\Gamma$ variables concerning the boundary Γ. This condensation leads to the compact algebraic linear equation

$$\int_{\Gamma_d} \mathbf{\Psi}^T_w(\boldsymbol{\xi})\mathbf{p}(\boldsymbol{\xi})\mathrm{d}\Gamma_\xi = \mathbf{P} = \tilde{\mathbf{Z}}\mathbf{W} - \mathbf{P}^E, \tag{18}$$

where we have set:

$$\tilde{\mathbf{Z}} = \mathbf{G}^{dd}_{pp} - \left\{\mathbf{G}^{ud}_{up} \quad -\mathbf{G}^{pd}_{pp}\right\}\mathbf{A}^{-1}\left\{\begin{array}{c}\mathbf{G}^{du}_{pu}\\ -\mathbf{G}^{dp}_{pp}\end{array}\right\}, \tag{19}$$

$$\mathbf{P}^E = \bar{\mathbf{G}}^d + \mathbf{A}^{-1}\left\{\begin{array}{c}\bar{\mathbf{G}}^u\\ \bar{\mathbf{G}}^p\end{array}\right\}, \quad \mathbf{A} = \left[\begin{array}{cc}\mathbf{G}^{uu}_{uu} & -\mathbf{G}^{pu}_{pu}\\ -\mathbf{G}^{up}_{up} & \mathbf{G}^{pp}_{pp}\end{array}\right]. \tag{20}$$

In Eq. $(20)_a$ $\mathbf{P}^E$ represents generalized tractions on Γ_d due to external actions in the absence of displacement discontinuities. Equations (16)–(20) give rise to the remarks that follow (partly anticipated in Sec. 1) intended to point out some distinct typical features of the SGBEM adopted herein.

(a) The coefficient matrix in Eq. (16) is symmetric, as a consequence of Betti's reciprocity Eq. (10) to be allowed for in the integrations (17). This symmetry directly implies the symmetry of matrices **A** and $\tilde{\mathbf{Z}}$ through their definitions by Eqs. (20) and (19).

(b) The three block-diagonal submatrices of coefficients in Eq. (16) are definite in sign. Specifically: $\mathbf{G}^{uu}_{uu}$ is positive definite; $\mathbf{G}^{pp}_{pp}$, $\mathbf{G}^{dd}_{pp}$ are negative definite, or at least semidefinite when the relevant locus, Γ_u or Γ_d, is such that rigid body motion is possible (with some distribution of kinematic variables on them). In fact, Eq. (17) shows that the meaning of the quadratic form associated to $\mathbf{G}^{uu}_{uu}$ is the elastic strain energy in Ω_∞ when it is acted by a force field on Γ_u; those associated to $\mathbf{G}^{pp}_{pp}$ and $\mathbf{G}^{dd}_{pp}$ and reversed in sign, represent energy in Ω_∞ due to distorsions (displacement jumps) in Γ_p and Γ_d, respectively, see e.g. [56, 57].

(c) Matrix **A** concerning boundary variables, Eq. $(20)_b$, is symmetric, as a principal submatrix of that in Eq. (16), but not semidefinite in sign. Its inverse exists whenever the original "linear background" b.v. problem, with $\mathbf{w} = \mathbf{0}$ in Γ_d and its BE discretization prevent rigid body motions and, hence, admit a unique solution both in stresses and displacements. The explicit inversion of **A** to condense all boundary variables and generate $\tilde{\mathbf{Z}}$, Eq. (19), is an option adopted herein, in order to derive both numerical simulations procedures and overall stability and bifurcation criteria in later Sections. As for the computational effort it requires, it is worth noting that the inversion of **A** is done once for all, as long as **A** depends on the boundary Γ and its modelling (not on locus Γ_d); moreover, it is made more economical by the symmetry compared to traditional BEMs, and by the reduced size of **A** compared to FEMs (which would require condensation of variables on both Γ_p and Ω).

(d) The influence coefficient matrix $\tilde{\mathbf{Z}}$ relating static generalized variables **W** on locus Γ_d to the static ones there, turns out to be symmetric because of its generation, Eq. (19), and negative

definite (semidefinite if material separation along Γ_d were to make rigid body motions possible). The latter property stems from the well expected energy meaning of its quadratic form (to within a change in sign, the strain energy in the given structure $\bar{\Omega}$, subjected to distorsions along Γ_d). Therefore we may write:

$$\tilde{\mathbf{Z}}^T = \tilde{\mathbf{Z}}; \qquad -\frac{1}{2}\mathbf{W}^T\tilde{\mathbf{Z}}\mathbf{W} \geq 0. \tag{21}$$

It is well stressing that, as anticipated in Sec. 1, the properties of the above discrete influence operator $\tilde{\mathbf{Z}}$ are the same as those of its continuum counterpart $\mathbf{Z}(\mathbf{x}, \boldsymbol{\xi})$, Eq. (2).

4. Double integrations of singular integrands

As mentioned in Sec. 1, a crucial step in the SGBEM is the choice and implementation of a sound procedure for the evaluation of the singular double integrals in Eqs. (7)–(9). Denoting by r the distance between the source point ξ and the "field point" $\mathbf{x}$ where effects are considered, and by $O(\cdot)$ the asymptotic behaviour for $r \to 0$ ($r \equiv [(\mathbf{x}-\boldsymbol{\xi})^T(\mathbf{x}-\boldsymbol{\xi})]^{1/2}$), the singularities of the Green functions employed are specified by the following tableau.

$$\begin{bmatrix} \mathbf{G}^{uu}\, O(\log r) \text{ in 2D, } O(1/r) \text{ in 3D} & \mathbf{G}^{pu}\, O(1/r^{D-1}) \\ \mathbf{G}^{up}\, O(1/r^{D-1}) & \mathbf{G}^{pp}\, O(1/r^{D}) \end{bmatrix}, \tag{22}$$

where $D = 2$ in 2D and $D = 3$ in 3D. According to a popular terminology, kernel $\mathbf{G}_{uu}$ is said to be weakly singular, $\mathbf{G}_{pu}$ and $\mathbf{G}_{up}$ strongly singular and $\mathbf{G}_{pp}$ hypersingular.

The issue of the mathematical meaning and evaluation of such integrals has been addressed in an abundant literature over the last few years. At least four ad-hoc procedures have been proposed in the general context of BEMs: (a) the singularity isolation, proposed in [30] and so far implemented only for collocation approaches; (b) the singularity subtraction technique developed in ([39]) based on suitable use of simple solutions; (c) particular quadrature rules ([16]) apt to the direct numerical computation in the spirit of customary Gauss formulae for nonsingular integrals but capturing Cauchy's principal values and Hadamard's finite parts in the presence of singularities; (d) the derivative transfer technique ([28, 61]).

Hereafter only the last method will be considered for the evaluation of hypersingular integrals, since it seems to be the best suited approach for the SGBEM. Details can be found in [28, 61]. The main ideas and the "Leitmotiv" of the derivative transfer technique can be outlined as follows, with reference to the hypersingular kernel $\mathbf{G}_{pp}$, to 2D problems and to the first implementations of the SGBEM in elasticity [61] and plasticity [49] (where linear BEs and linear shape functions were adopted, in [61] with a complex variable formalism): (i) express $\mathbf{G}_{pp}$ in terms of first derivatives, with respect to each of two curvilinear coordinates over BEs, of an auxiliary kernel $\mathbf{G}_{\varphi\varphi}$, according to an interpretation of $\mathbf{G}_{pp}$ proposed in ([55]); (ii) integrate twice by parts the integrand, thus transferring the derivatives to the interpolation functions, chosen so that they make the generated nonintegral terms vanish; (iii) perform, numerically or analytically, the weakly singular integration of the remaining integral term containing the auxiliary kernel $\mathbf{G}_{\varphi\varphi}$. A general mathematical description of this "regularization" technique by the derivative transfer is given below (cf. [14, 28]).

Let us consider, in tensorial notation, the integral over any Γ (surface in 3D or curve in 2D):

$$\mathcal{I} = \int_\Gamma \int_\Gamma \Psi_u^i(\boldsymbol{\xi}) G_{pp}^{ik}(\mathbf{x}, \boldsymbol{\xi}) \Psi_u^k(\mathbf{x}) \mathrm{d}\Gamma_x \mathrm{d}\Gamma_\xi, \tag{23}$$

where shape functions $\Psi_u^i(\boldsymbol{\xi})$ and $\Psi_u^k(\mathbf{x})$ defined over Γ are assumed to be continuous and to vanish on the boundary $\partial\Gamma$ of Γ. It can be shown ([14]) that

$$G_{pp}^{ik}(\mathbf{x}, \boldsymbol{\xi}) = R_\xi^j R_x^q [G_{\varphi\varphi}^{ijkq}(\mathbf{x}, \boldsymbol{\xi})], \tag{24}$$

where $G^{ijkq}_{\varphi\varphi}(\mathbf{x},\boldsymbol{\xi})$ is a weakly singular kernel to be defined later and R^q_x, R^j_ξ are the surface rotor operators at $\mathbf{x}$ and $\boldsymbol{\xi}$, respectively. Considering the scalar field $g(\mathbf{x})$ ($f(\boldsymbol{\xi})$, respectively), and denoting by $\mathbf{n}$ ($\mathbf{m}$) the normal versor to Γ at $\mathbf{x}$ ($\boldsymbol{\xi}$), R^q_x (R^j_ξ) is the projection on $\mathbf{n}$ ($\mathbf{m}$) of the rotor of vector $g(\mathbf{x})\mathbf{e}_j$ ($f(\boldsymbol{\xi})\mathbf{e}_q$), $\mathbf{e}_j$ being the j^{th} coordinate-axis versor, i.e.

$$R^q_x[g(\mathbf{x})] = e_{qrs}\frac{\partial g(\mathbf{x})}{\partial x_s}n_r, \qquad R^j_\xi[f(\boldsymbol{\xi})] = e_{jrs}\frac{\partial f(\boldsymbol{\xi})}{\partial \xi_s}m_r, \tag{25}$$

where and e_{jrs} is the permutation symbol ($e_{jrs}\neq 0$ for $j\neq r\neq s$, $e_{jrs}=1$ for $\{j,r,s\}=\{1,2,3\}$ or any even permutation of it, $e_{jrs}=-1$ otherwise). The surface rotors in Eq. (25) can be expressed in terms of surface derivatives of shape functions, e.g.:

$$R^q_x[g(\mathbf{x})] = e_{qrs}\frac{\partial g(\mathbf{x})}{\partial x_s}n_r = \left(\frac{\partial g(\mathbf{x})}{\partial \eta_1}a^q_2 - \frac{\partial g(\mathbf{x})}{\partial \eta_2}a^q_1\right)J^{-1}(\eta_1,\eta_2), \tag{26}$$

where: η_1 and η_2 are the "master element" coordinates on Γ at $\mathbf{x}$; $\mathbf{a}_1$ and $\mathbf{a}_2$ are the relevant covariant base vectors and J the jacobian of the transformation $x_i = x_i(\eta_1,\eta_2)$. In 2D (where $j\equiv q\equiv 3$) if ℓ_x and ℓ_ξ are the arc length coordinates along Γ related to $\mathbf{x}$ and $\boldsymbol{\xi}$, the surface rotor operators reduce to the derivative with respect to ℓ_x and ℓ_ξ, respectively, i.e.

$$R^3_x[g(\mathbf{x})] = \frac{\partial g}{\partial \eta_x}J^{-1}(\eta_x) = \frac{\partial g}{\partial \ell_x} \quad \text{and} \quad R^3_\xi[f(\boldsymbol{\xi})] = \frac{\partial f}{\partial \eta_\xi}J^{-1}(\eta_\xi) = \frac{\partial f}{\partial \ell_\xi}. \tag{27}$$

Integration by parts of Eq. (23) making use of Eqs. (24) (25), transfers the derivatives to the shape functions:

$$\mathcal{I} = \int_\Gamma\int_\Gamma R^j_\xi[\Psi^i_u(\boldsymbol{\xi})]G^{ijkq}_{\varphi\varphi}(\mathbf{x},\boldsymbol{\xi})R^q_x[\Psi^k_u(\mathbf{x})]\mathrm{d}\Gamma_x\mathrm{d}\Gamma_\xi. \tag{28}$$

It should be stressed that properties (26)(27) represent a prominent feature of the surface rotor operator, according to which $R^q_x[\Psi^k_u(\mathbf{x})]$ and $R^j_\xi[\Psi^i_u(\boldsymbol{\xi})]$ can be computed by just differentiating $\Psi^k_u(\mathbf{x})$ and $\Psi^i_u(\boldsymbol{\xi})$ with respect to coordinates lying in the domain of definition of the shape functions themselves.

In 2D, setting $G^{ik}_{\varphi\varphi}(\mathbf{x},\boldsymbol{\xi}) \equiv G^{i3k3}_{\varphi\varphi}(\mathbf{x},\boldsymbol{\xi})$

$$G^{ik}_{pp}(\mathbf{x},\boldsymbol{\xi}) = \frac{\partial}{\partial \ell_\xi}\frac{\partial}{\partial \ell_x}[G^{ik}_{\varphi\varphi}(\mathbf{x},\boldsymbol{\xi})] \tag{29}$$

while Eq. (28) becomes

$$\mathcal{I} = \int_\Gamma\int_\Gamma \frac{\partial \Psi^i_u(\boldsymbol{\xi})}{\partial \ell_\xi}G^{ik}_{\varphi\varphi}(\mathbf{x},\boldsymbol{\xi})\frac{\partial \Psi^k_u(\mathbf{x})}{\partial \ell_x}\mathrm{d}\Gamma_x\mathrm{d}\Gamma_\xi. \tag{30}$$

The explicit expression for the $G^{ikjp}_{\varphi\varphi}$ kernel in the general 3D case, as put forward in [55], reads

$$G^{ijkq}_{\varphi\varphi}(\mathbf{x},\boldsymbol{\xi}) = \mu^2 e_{ibe}e_{kgs}A_{ejsq}\frac{\partial}{\partial x_b}\frac{\partial}{\partial \xi_g}[F(\mathbf{x},\boldsymbol{\xi})], \tag{31}$$

where, denoting by μ the shear modulus, it has been set:

$$F \equiv -\frac{1}{16\pi\mu(1-\nu)}r^2\log r \quad \text{in 2D}, \qquad F \equiv \frac{1}{16\pi\mu(1-\nu)}r \quad \text{in 3D},$$

$$A_{ejsq} \equiv 4\nu\delta_{ej}\delta_{sq} + 2(1-\nu)(\delta_{eq}\delta_{js} + \delta_{es}\delta_{jq}). \tag{32}$$

By specializing Eq. (32) to the 2D case ([28, 61]), namely by assuming $e \equiv s \equiv j \equiv q \equiv 3$, and denoting by Δ the Laplacian operator, we have:

$$G^{ik}_{\varphi\varphi}(\mathbf{x},\boldsymbol{\xi}) \equiv G^{i3k3}_{\varphi\varphi}(\mathbf{x},\boldsymbol{\xi}) = -4\mu^2 \left[\delta_{ik}\Delta F(\mathbf{x},\boldsymbol{\xi}) - \frac{\partial}{\partial x_i}\frac{\partial}{\partial x_k}[F(\mathbf{x},\boldsymbol{\xi})]\right]$$

$$= \frac{\mu}{2\pi(1-\nu)}\left[\log r\delta_{ik} - \frac{\partial r}{\partial x_i}\frac{\partial r}{\partial x_k}\right]. \tag{33}$$

The main advantages displayed by this regularized formulation can be summarized as follows.

(i) Equations (28) and (30) contain now only weakly singular integrals which do not require complicated interpretations (i.e. Cauchy's principal values or Hadamard's finite parts).

(ii) Integrals in Eqs. (28) and (30) can be evaluated numerically by means of standard and reliable numerical quadrature rules, since every single term in the kernels displays at most weak singularities (not only the global expression as in the singularity subtraction technique).

(iii) Explicit expressions of regularized kernels $G_{\varphi\varphi}$ (see Eq. (33) in particular) are easier to compute than the lengthy explicit expression of G_{pp}, not reported here for brevity (actually $G^{ik}_{pp} = E_{ijab}E_{kpcd}(\partial^2/\partial x_b \partial\xi_d)G^{ac}_{uu}n_j m_p$, with E elastic stiffness tensor).

5. Analytical description of path-dependent cohesive crack models

In what precedes the linear background of the fracture mechanics problem has been fully described, in the sense that all elastic and geometrical properties of the structure in point and the external actions have been allowed for in formulating the "symmetric" integral equations (BIEs) over the boundary Γ and the displacement discontinuity locus Γ_d, Sec. 2, Eqs. (7)–(9). The Galerkin discretization and subsequent condensation of the boundary variables, led to the linear relationship, Eq. (18), through the elastic structure, between displacement jumps $\mathbf{w}$ and tractions $\mathbf{p}$ along Γ_d. The SGBEM has been discussed as a general and computationally attractive procedure leading to a discrete approximation of Eq. (2) for the structure in point, originally interpreted as a solid continuum contained in $\bar{\Omega}$.

In order to complete the problem formulation the variables $\mathbf{w}$ and $\mathbf{p}$ on Γ_d are now to be linked through a constitutive model apt to interpret, at an engineering-oriented phenomenological level, the nonlinear mechanical events, in primis the fracture processes, confined to Γ_d by the basic assumption of cohesive-crack models.

For a unified analytical description of most interface constitutions adopted in the literature, see e.g. [17, 19, 31, 34, 38, 42, 59, 62, 64, 65], we borrow from plasticity, e.g. [7, 43], and continuum damage mechanics, [41], the following formulation based on concepts and symbols specified below:

$$\mathbf{w} = \mathbf{w}^e + \mathbf{w}^p, \tag{34}$$

$$\mathbf{p} = \frac{\partial \pi}{\partial \mathbf{w}^e}(\mathbf{w}^e, \mathbf{s}), \qquad \mathbf{q} = \frac{\partial \pi}{\partial \mathbf{s}}(\mathbf{w}^e, \mathbf{s}), \tag{35}$$

$$\dot{\mathbf{w}}^p = \frac{\partial \hat{\phi}}{\partial \mathbf{p}}^T(\mathbf{p},\mathbf{q})\dot{\boldsymbol{\lambda}}, \qquad \dot{\mathbf{s}} = -\frac{\partial \hat{\phi}}{\partial \mathbf{q}}^T(\mathbf{p},\mathbf{q})\dot{\boldsymbol{\lambda}}, \tag{36}$$

$$\dot{\boldsymbol{\lambda}} \geq 0, \qquad \boldsymbol{\phi}(\mathbf{p},\mathbf{q}) \leq 0, \qquad \boldsymbol{\phi}^T\dot{\boldsymbol{\lambda}} = 0. \tag{37}$$

The displacement discontinuity $\mathbf{w}$ across Γ_d is assumed, through Eq. (34), as the sum of an elastic $\mathbf{w}^e$ and an irreversible (permanent or plastic) part $\mathbf{w}^p$. Internal variables in conjugate pairs, gathered in vectors $\mathbf{s}$ of the kinematic and $\mathbf{q}$ of the static ones, are intended to reflect, at the macroscale, dissipative phenomena. For concrete-like materials, fracture results from complex phenomena occurring in a "process zone" in the vicinity of Γ_d (or of parts of it), at the micro- and

meso-levels (such as microcracks and local plastic yielding related to the inhomogeneous texture of "disordered" materials consisting of aggregates, matrix and interfaces).

In Eq. (35) a potential π (assumed as twice differentiable at least) represents the recoverable ("free" Helmholtz's) energy (per unit volume), encompassing the elastic strain energy π^E (if any) and the energy π^L locked in the materials by rearrangements at the microscale reflected by $\mathbf{s}$. Both addends (not only the latter) are thought of as functions of the kinematic internal variables $\mathbf{s}$, so that interface damage in the sense of elastic stiffness degradation can be allowed for, where desirable. Plastic potentials $\hat{\phi}$ are adopted to describe in rates through Eq. (36) the evolution of both $\mathbf{w}^p$ and $\mathbf{s}$ by their gradients and non-decreasing plastic multipliers $\boldsymbol{\lambda}$. The yield criterion is formulated in Eq. $(37)_b$ by means of a vector $\boldsymbol{\phi}$ of convex differentiable yield functions, the argument of which contain, besides the traction $\mathbf{p}$ across Γ, the static internal variables $\mathbf{q}$ in order to describe hardening or softening (softening understood here as shrinking of the elastic domain). Vectors $\boldsymbol{\phi}$ and $\hat{\boldsymbol{\phi}}$ are assumed with same dimensionality and as convex functions of $(\mathbf{p}, \mathbf{q})$. They are generally distinct, to reflect frictional behaviour by lack of normality (nonassociativity) in the $\mathbf{p}$ and $\dot{\mathbf{w}}^p$ spaces superposed and/or in the $\mathbf{q}$ and $\dot{\mathbf{s}}$ spaces superposed.

Equation (37) (called in plasticity Prager's loading-unloading rule or "consistency" rule) requires ortoghonality of vectors $\boldsymbol{\phi}$ and $\dot{\boldsymbol{\lambda}}$, but holds also componentwise (i.e. $\phi_i \dot{\lambda}_i = 0$, $\forall i$), in view of their sign constraints. A dot means derivative with respect to any strictly monotonically increasing function t of chronological time, in view of the inviscid nature assumed for the mechanical processes in point.

As an illustration, consider the simplest, frequently used CCM for mode I shown in Fig. 1a. It is readily seen to be covered by Eqs. (34)-(37) as a very special case for: $w^e = 0$, $\hat{\phi} = \phi = p - (p_C + hw)$, $\pi = p_C s + 1/2 h w^2$; whence $q = p_C + hw$, $w = \lambda = s$, $h < 0$ being the modulus of linear softening. Clearly, for $w > w_c$ (i.e. $q > 0$) actual crack arises and the above nonholonomic description no longer holds ($\mathbf{p} = 0$, uncorrelated to $\mathbf{w}$).

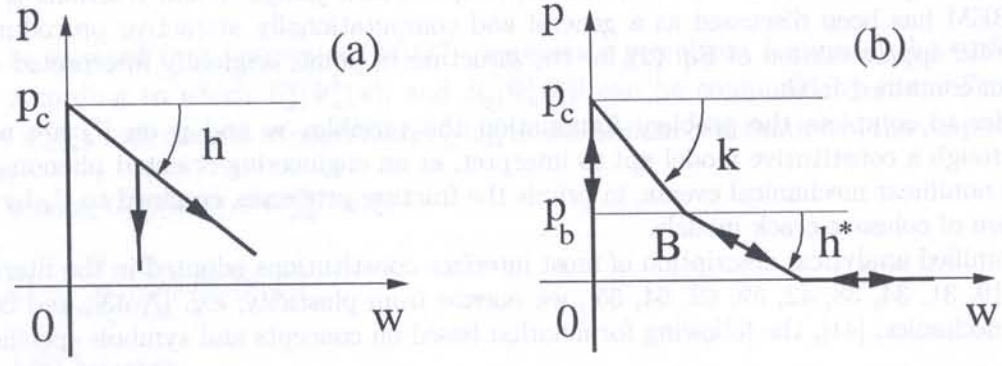

Fig. 1. Mode I, piecewise-linear cohesive crack models: (a) nonholonomic, (b) holonomic with break point B

Let us derive from Eqs. (34)–(37) the relation in rates (dotted variables), i.e. in infinitesimal increments (to within a common time increment δt). Equations (37) discriminate the inactive yield modes (those for which $\phi_i < 0$ and hence $\dot{\lambda}_i = 0$) from those (with $\phi_j = 0$ at t) which may be activated (i.e. $\dot{\lambda}_i \geq 0$) in rate processes starting from the state t. Marking by primes the vectors $(\boldsymbol{\phi}', \hat{\boldsymbol{\phi}}', \boldsymbol{\lambda}')$ of variables pertaining only to the modes which can be activated and by bars the known values of all variables at time t, the rate relations straightforwardly flow from Eqs. (34)–(37):

$$\dot{\mathbf{w}} = \dot{\mathbf{w}}^e + \dot{\mathbf{w}}^p, \tag{38}$$

$$\begin{Bmatrix} \dot{\mathbf{p}} \\ \dot{\mathbf{q}} \end{Bmatrix} = \begin{bmatrix} \mathbf{k}_e & \mathbf{k}_{es} \\ \mathbf{k}_{se} & \mathbf{k}_s \end{bmatrix} \begin{Bmatrix} \dot{\mathbf{w}}^e \\ \dot{\mathbf{s}} \end{Bmatrix}, \tag{39}$$

$$\dot{\mathbf{w}}^p = \frac{\partial \hat{\phi}'^T}{\partial \mathbf{p}}(\bar{\mathbf{p}}, \bar{\mathbf{q}})\dot{\lambda}', \qquad \dot{\mathbf{s}} = -\frac{\partial \hat{\phi}'^T}{\partial \mathbf{q}}(\bar{\mathbf{p}}, \bar{\mathbf{q}})\dot{\lambda}', \tag{40}$$

$$\dot{\lambda}' \geq 0, \qquad \dot{\phi}' = \frac{\partial \phi'}{\partial \mathbf{p}^T}\dot{\mathbf{p}} + \frac{\partial \phi'}{\partial \mathbf{q}^T}\dot{\mathbf{q}} \leq 0, \qquad \dot{\phi}'^T \dot{\lambda}' = 0. \tag{41}$$

In Eq. (39) the Hessian matrix of the potential $\pi(\mathbf{w}^e, \mathbf{s})$ is partitioned into submatrices $\mathbf{k}$, of which the instantaneous (tangent) elastic stiffnesses read:

$$\mathbf{k}_e = \frac{\partial^2 \pi}{\partial \mathbf{w}^e \partial \mathbf{w}^{eT}}(\bar{\mathbf{w}}^e, \bar{\mathbf{s}}), \qquad \mathbf{k}_s = \frac{\partial^2 \pi}{\partial \mathbf{s} \partial \mathbf{s}^T}(\bar{\mathbf{w}}^e, \bar{\mathbf{s}}). \tag{42}$$

The energy dissipation rate (first-order external work minus free energy rate) must comply with the thermodynamical requirement:

$$\dot{D} = \frac{\delta^1 \mathcal{L}}{\delta t} - \dot{\pi} = \mathbf{p}^T \dot{\mathbf{w}} - \left(\frac{\partial \pi}{\partial \mathbf{w}^{eT}} \dot{\mathbf{w}}^e + \frac{\partial \pi}{\partial \mathbf{s}^T} \dot{\mathbf{s}} \right) \geq 0. \tag{43}$$

Constitutive stability is understood here not in the more restrictive sense of Drucker [43], but in the sense of no tendency to spontaneously quit the current state. According to a classical concept, see e.g. [7, 43, 44], (statical) stability in this sense means semi-positiveness of the second-order work $\delta^2 \mathcal{L}$ performed by an external energy which promotes any kinematic disturbance (here $\delta \mathbf{w}$) while providing the static actions to preserve the balance between internal and external static quantities. In symbols:

$$\delta^2 \mathcal{L} = \frac{1}{2} \dot{\mathbf{p}}^T(\dot{\mathbf{w}}) \dot{\mathbf{w}} \delta t^2 \geq 0, \qquad \forall \dot{\mathbf{w}}. \tag{44}$$

Making use of Eqs. (39)-(41), the second order work can be given the expression:

$$\begin{aligned} \delta^2 \mathcal{L}\, 2(\delta t^{-2}) = {} & \dot{\mathbf{w}}^{eT} \mathbf{k}_e \dot{\mathbf{w}}^e + \dot{\lambda}'^T \frac{\partial \phi'}{\partial \mathbf{q}^T} \mathbf{k}_s \frac{\partial \hat{\phi}'^T}{\mathbf{q}} \dot{\lambda}' \\ & + \dot{\mathbf{w}}^{eT} \left[\mathbf{k}_e \frac{\partial}{\partial \mathbf{p}} (\hat{\phi}' - \phi')^T - \mathbf{k}_{es} \frac{\partial}{\partial \mathbf{q}} (\hat{\phi}' + \phi')^T \right] \dot{\boldsymbol{\lambda}} \\ & + \dot{\lambda}'^T \frac{\partial \phi'}{\mathbf{q}^T} \mathbf{k}_{se} \frac{\partial}{\mathbf{p}} (\hat{\phi}' - \phi')^T \dot{\lambda}'. \end{aligned} \tag{45}$$

It is worth noting that the matrix [in square brackets] of the bilinear form in Eq. (45) consists of two addends: the former arises from nonassociativity ($\hat{\phi} \neq \phi$), the latter from damage in the sense of elastic behaviour influenced by internal variables (potential π^e depending on both $\mathbf{w}^e$ and $\mathbf{s}$, so that $\mathbf{k}_{es} \neq \mathbf{0}$. The cooperative effects of elastic-plastic coupling (or damage) and lack of normality on the flow laws of elastoplasticity have been pointed out and investigated in [45]. Though not corroborated by physical arguments and often disproved by experiments on interface behaviour, associativity, $\hat{\phi} = \phi$, and no damage, $\pi^e(\mathbf{w}^e)$, are frequently assumed in the literature and will be adopted henceforth herein in view of the remarkable simplification this assumption implies and the insight it permits. In fact, for associated flow rules and no elastic-plastic coupling, the last two addends in Eq. (45) vanish and the above sufficient and necessary stability criterion can be given an easy and meaningful interpretation, since, when $\hat{\phi} = \phi$ and $\mathbf{k}_{es} = \mathbf{0}$, Eq. (45) reduces to:

$$\delta^2 \mathcal{L}\, 2(\delta t)^{-2} = \dot{\mathbf{w}}^{eT} \mathbf{k}_e \dot{\mathbf{w}}^e + \dot{\lambda}'^T \frac{\partial \phi'}{\partial \mathbf{q}^T} \mathbf{k}_s \frac{\partial \phi'^T}{\partial \mathbf{q}} \dot{\lambda}'. \tag{46}$$

What precedes, centered on Eqs. (34)–(37), gives rise to the following remarks.

(a) When the elastic addend $\mathbf{w}^e$ of displacement discontinuity is accommodated in the model, the potential π is assumed strictly convex in $\mathbf{w}^e$ (and usually quadratic), i.e. the tangent stiffness matrix $\mathbf{k}_e$ is positive definite (and in particular independent from $\mathbf{w}_e$, which means linear elasticity). The internal variable vector $\mathbf{s}$ often affects $\mathbf{k}_s$ through its (isotropic) damage variable D in the stiffness degradation factor $1 - D$, which does reflect observable aspects in some quasi-brittle processes, see e.g. [11, 23, 41, 59]. In most CCM, however, (and in what follows) damage in this sense is not considered and, as mentioned above, decoupling is assumed in the free energy potential: $\pi = \pi^E(\mathbf{w}^e) + \pi^L(\mathbf{s})$ (so that $\mathbf{k}_{es} = \mathbf{k}_{se}^T = 0$). Quadratic locked-in energy $\pi^L(\mathbf{q})$ implies linear hardening or softening. Frequently adopted is the rigid-plastic CCM (and interface model), covered by the specializations: $\mathbf{w}^e = \mathbf{0}$ (and, hence, $\pi^E = 0$) and $\mathbf{p}$ uncorrelated to $\mathbf{w}^e$.

(b) For associative rigid-plastic ($\mathbf{w}^e = \mathbf{0}$) models, in view of Eq. (46), the constitutive stability criterion, Eq. (44), in associative cases leads directly to the conclusion: sufficient condition for the cohesive crack model (CCM) to be stable is the positive semidefiniteness of matrix $\mathbf{k}_s$ (see in Eq. (46), the latter addend), i.e. the convexity of the free energy potential π in the kinematic internal variables $\mathbf{s}$, see Eq. $(42)_b$. Therefore concavity of π in $\mathbf{s}$ is necessary for the constitutive instability, i.e. for the softening behaviour. Softening is the central feature of the CCMs of concern herein, since it represents damage in the sense of strength reduction up to material decohesion.

(c) In the rate formulation, Eqs. (38)-(41), of the general CCM, other issues would be of interest, such as criteria for uniqueness (or lack thereof) of the response to given $\dot{\mathbf{w}}$ and the concept of Hill's "linear comparative solid" (see e.g. [11]). However, these issues are not discussed here, in view of the mathematical analogies with familiar damage-plasticity constitutive theory (in terms of strain-stress tensor instead of vectors $\mathbf{w}$ and $\mathbf{p}$) and with subsequent developments concerning the overall structural behaviour (Sec. 10).

(d) Within Γ_d, *a priori* defined in Ω as the locus of potential or actual displacement jumps, three portions must be distinguished at an instant t, in order to properly formulate a boundary value problem in rates over $\bar{\Omega}$: (i) crack (or union of cracks) Γ_d^c, where no interaction exists ($\mathbf{p} = \mathbf{0}$) and $\dot{\mathbf{w}}$ cannot be correlated to $\dot{\mathbf{p}}$; (ii) undamaged elastic material Γ_d^e, where $\dot{\boldsymbol{\lambda}}(\tau) = 0$ for any $0 \leq \tau \leq t$ (assuming that $\Gamma_d^e \equiv \Gamma_d$ at time $t = 0$); (iii) process zone Γ_d^p, in each point of which $\mathbf{p} \neq \mathbf{0}$ and at least one yield mode can be activated (say the i^{th} : $\phi_i = 0$). Other local situations are assumed to occur only on borders of transition between the above subloci, i.e. on parts of Γ_d with lesser dimensionality compared to Γ_d. It is understood that the process zone Γ_d^p includes possible parts of Γ_d where contact (between two faces, say Γ_d^+ and Γ_d^-) has been restored after a crack has been generated: in fact, frictional contact can be reasonably described by suitable specializations of Eqs. (34)–(37), see e.g. [50].

(e) In modelling interface behaviour, especially contact with friction and interlocking of asperities of crack faces, associativity represents a dubious compromise between conflicting requirements of computational simplicity and cost-effectiveness on one side and realism on the other. It can be noticed, however, that some of the most undesirable consequences, such as excessive dilatancy, may be attenuated, in an overall average sense, by the provision of multiple yielding modes. A popular example of this fact in soil and concrete plasticity is provided by Drucker-Prager model "improved" by a "cap" which becomes active for predominantly compressive states.

(f) The history-dependent (or irreversible, or "nonholonomic") character of the class of models considered so far is quite apparent in Eqs. (34)-(37). For evolutive ("marching") numerical solutions of the nonlinear initial boundary value problem over $\Omega \times T$ (T being the time interval of interest), the approximation by a sequence of (still nonlinear) boundary-value (no longer initial-value) step-problems is practically unavoidable. This means that, for the finite step problem, say over $\Delta t = [t_n, t_{n+1}]$, assuming as known (and, hence, by marking by bars) all variables at t_n, a step-wise holonomic version of it must be derived from the non-holonomic model Eqs. (34)-(37). This version can be generated, e.g., according to the implicit backward-difference time-integration scheme well known in plasticity, see e.g. [20, 43]) . Clearly, if the time step Δt coincides with the whole interval T, a fully holonomic (i.e. nonlinear-elastic) model is arrived at, but this is not computationally advisable (inaccuracy and, with softening, algorithmic instabilities increase with the step size).

When single-step holonomic analysis is legitimate, and advantageous to engineering purposes, *ad hoc* holonomic CCMs are suitable. Some of them are formulated in Sec. 6.

6. HOLONOMIC COHESIVE CRACK MODELS

In a number of engineering situations, especially when the main external actions can be interpreted as varied by a load factor monotonically increasing in time, manifestations of irreversibility (such as "local unloading") can *a priori* be conjectured to play a minor role, if any, in the overall structural response. In such situations, nonlinear material behaviours which actually are dissipative, (i.e. history-dependent, nonholonomic) may be interpreted as reversible (i.e. holonomic) to structural analysis purposes. Then in the present context of nonlinear fracture mechanics, when the locus Γ_d of possible displacement discontinuities (in particular, the crack propagation itinerary) can be reasonably assumed *a priori*, structural responses implying fracture processes can be predicted by single-step computations based on holonomic CCMs (in total variables), rather than by time-stepping evolutive analysis, with obvious potential savings.

In order to discuss some typical aspects of non-evolutive simulations of quasi-brittle fractures, we will focus first on the CCM for mode I processes depicted in Fig. 1_b. The reasons of the interest in this particular CCM are as follows: (a) the bilateral softening branch (with break-point B) has been found to approximate well accurate experimental results concerning concrete like materials and seems to be advocated by several researchers in the field, e.g. [2, 65]; (b) its piecewise linear (PWL) nature, besides possible advantages in marching solutions (Sec. 9), permits recourse to special ad hoc algorithms with novel theoretical and computational features (Sec. 10); (c) the nontraditional analytical description presented below in terms of a linear complementarity problem (LCP) is analogue to the one typical of the rate relations of Sec. 5, and encompasses as a special case the linear softening branch, so that some formal unification can be achieved.

The dependence visualized in Fig. 1_b of normal tractions $\mathbf{p} = p\mathbf{n}$ ($\mathbf{n}$ being the normal to locus Γ_d assumed smooth) on opening displacement $\mathbf{w} = w\mathbf{n}$ (in $2D$ problems) is defined by four material parameters. These are, e.g the tensile strength of concrete p_C; the coordinates w_B, p_B of the "break point" B; the "critical" opening displacement w_c, above which the two faces (Γ_d^+ and Γ_d^-) do not interact (or the fracture energy $\mathcal{G}_I$, i.e. the area defined by the plot). Alternative choices of the four parameters are: p_C, p_B, k, h^* (k and h^* being the negative slopes of the two descending branches in Fig. 1_b; p_C, p_B, h_1, h, having set $h = kh^*(k - h^*)^{-1}$. The last choice is preferred here since it simplifies the analytical formulation. Interpreted as holonomic, the CCM depicted in Fig. 2_b is a nonsmooth multivalued dependence $p(w)$ or $w(p)$, which can easily be defined in a descriptive way, interval by interval, but not by a single function. A mathematical model, which provides a suitable basis for theoretical and computational developments, can be generated by means of auxiliary variables ϕ_1, ϕ_2, ϕ_3, λ_1, λ_2 and represented as follows:

$$\begin{Bmatrix} \phi_1 \\ \phi_2 \\ \phi_3 \end{Bmatrix} = - \begin{bmatrix} k+h & k & -k \\ k & k & -k \\ k & k & -k \end{bmatrix} \begin{Bmatrix} \lambda_1 \\ \lambda_2 \\ w \end{Bmatrix} + p \begin{Bmatrix} 0 \\ 0 \\ 1 \end{Bmatrix} - \begin{Bmatrix} p_C - p_B \\ p_C \\ p_C \end{Bmatrix} \leq 0, \tag{47}$$

$$\{\lambda_1, \lambda_2, w\}^T \geq \mathbf{0}, \qquad \phi_1\lambda_1 + \phi_2\lambda_2 + \phi_3 w = 0. \tag{48}$$

The fact that Eq. (47) is an analytical representation of the graph of Fig. 1_b in the inverse (compliance) direction $w(p)$, can be easily proved or checked by inspection. This may be facilitated by the mechanical interpretation of the CCM as a combination in parallel (at any point of Γ_d, per unit surface, in its normal direction) of an arrestor which forbids overlapping ($w \leq 0$) and an unstable spring which is pre-stretched by force p_C for $w = 0$ and is endowed with piecewise constant (negative or zero) stiffness. Still preserving its LCP format, Eq. (47) might be rearranged so that the matrix in the linear equation between complementary variables becomes symmetric (whereas its lack of sign definiteness is an unchangeable essential feature of the LCP in point). The same path

of reasoning which led to the (LCP) description, Eqs. (47)–(48), of the PWL model with break point, Fig. 1b, leads to the one of the more popular CCM with a single linear descending branch (which could also be described by a specialization of Eq. (47) for $h \to -\infty$). Recently, a nonlinear complementarity problem (NLCP) format was proposed in [63] to describe a CCM for mode I with generally curved convex softening branch.

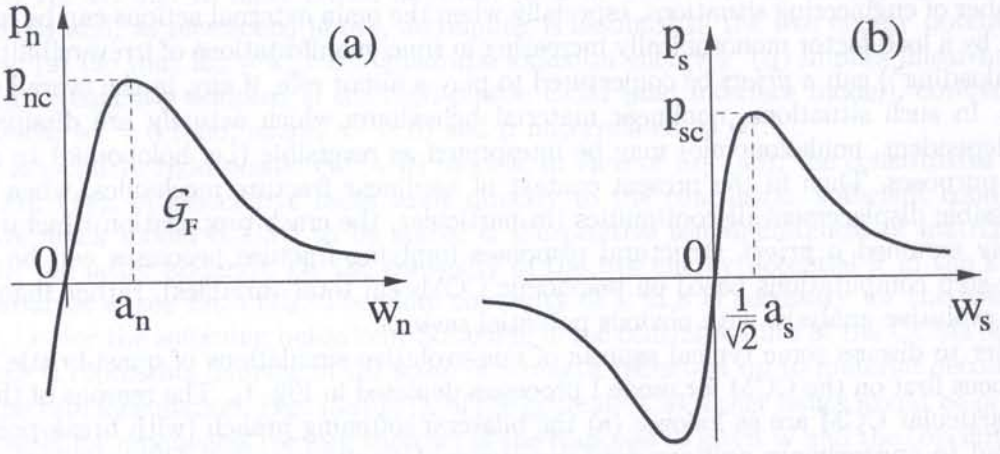

Fig. 2. Mixed mode, holonomic cohesive crack model [66]: (a) normal traction only ($p_s = 0$), (b) shear only ($p_n = 0$).

For mixed mode fracture processes PWL-LCP models are no longer practical and recourse to other mathematical constructs is suitable. For example, for 2D situations in which non negligible shear tractions must be expected on the discontinuity locus Γ_d, a holonomic CCM (Fig. 2) has been proposed in [66] (for simulations of quasi-brittle fracture processes in dynamics) in the following form:

$$p_n = \mathcal{G}_F a_n^{-1} \frac{w_n}{a_n} \exp\left(-\frac{w_n}{a_n}\right) \exp\left(-\left(\frac{w_s}{a_s}\right)^2\right), \tag{49}$$

$$p_s = 2\mathcal{G}_F a_s^{-1} \left(1 + \frac{w_n}{a_n}\right) \frac{w_s}{a_s} \exp\left(-\frac{w_n}{a_n}\right) \exp\left(-\left(\frac{w_s}{a_s}\right)^2\right). \tag{50}$$

where subscripts n and s refer to the normal and the tangential direction with respect to the locus Γ_d (assumed smooth) and the material parameters $\mathcal{G}_F$, a_n, a_s have the following meaning: $\mathcal{G}_F$ is the fracture energy in mode I; a_n represents the abscissa of the peak of $p_n(w_n)$ for $w_s = 0$; a_n is $\sqrt{2}$ times larger than the peak abscissa of $p_s(w_s)$ for $w_n = 0$. Pros of this kind of CCM are their analytical representation by simple functions. As cons, only increasing stiffness opposes overlapping faces on Γ_d (unless $w_n \geq 0$ is imposed explicitly) and face interaction vanishes asymptotically only.

7. Cohesive crack models in generalized variables

In Sec. 2 the unknown work-conjugate fields of displacement jumps $\mathbf{w}(\mathbf{x})$ and tractions $\mathbf{p}(\mathbf{x})$ along the discontinuity locus Γ_d, have been involved in the formulation of symmetric BIEs, Eq. (7). The Galerkin discretization of these equations and the condensation of all the boundary unknowns $\mathbf{P}_\Gamma$ and $\mathbf{W}_\Gamma$ have related through linear elasticity the Galerkin weighted averages $\mathbf{P}$ of the tractions across Γ_d to the generalized variables $\mathbf{W}$ governing the modelled field of displacement discontinuities along Γ_d. Vectors $\mathbf{W}$ and $\mathbf{P}$ originated from the expressions (in this section modelled fields will be marked by a tilde):

$$\tilde{\mathbf{w}}(\mathbf{x}) = \boldsymbol{\Psi}_w(\mathbf{x})\mathbf{W}, \qquad \mathbf{P} = \int_{\Gamma_d} \boldsymbol{\Psi}_w^T(\mathbf{x})\mathbf{p}(\mathbf{x})\mathrm{d}\Gamma_x. \tag{51}$$

In order to formulate a solvable space-discrete problem, the same variables $\mathbf{P}$ should now be related to $\mathbf{W}$ through the constitutive law adopted on Γ_d. To this purpose, it is fruitful to choose interpolations $\boldsymbol{\Psi}_p(\mathbf{x})$ through which tractions on Γ_d are governed by vector $\mathbf{P}$, Eq. $(51)_b$, and which comply with the requirements discussed below.

If the CCM is non-holonomic (physically it is always so), the basic, core problem has to be formulated in terms of rates (i.e., after space modelling in terms of ordinary differential equations and inequalities). This formulation will be referred to below. Clearly, the modelled traction rates $\dot{\tilde{\mathbf{p}}}$ defined by vector $\dot{\mathbf{P}}$ computed through elasticity by the SGBEM on the basis of a given vector $\dot{\mathbf{W}}$, will generally not coincide with the traction rates, say $\dot{\mathbf{p}}(\dot{\tilde{\mathbf{w}}})$, computed through the locally imposed CCM from the field $\dot{\tilde{\mathbf{w}}}$ defined by the same given $\dot{\mathbf{W}}$. Therefore, in order to relate $\dot{\tilde{\mathbf{p}}} = \boldsymbol{\Psi}_p \dot{\mathbf{P}}$ to $\dot{\tilde{\mathbf{w}}}$ through the mechanical behaviour of a locus of possible discontinuities, the CCM has to be enforced in an approximate, average sense.

In Sec. 5 the scalar product $\dot{\mathbf{p}}^T(\dot{\mathbf{w}})\dot{\mathbf{w}}$ proportional to the local second-order work density $\delta^2\mathcal{L}$, Eq. (45), has been related to the important concept of constitutive stability. It is therefore natural to adopt for modelling $\tilde{\mathbf{p}}$ shape functions $\boldsymbol{\Psi}_p$ which "preserve the dot product" (and its energy meaning), i.e. such that:

$$\dot{\mathbf{P}}^T\dot{\mathbf{W}} = \int_{\Gamma_d} \dot{\tilde{\mathbf{p}}}^T \dot{\tilde{\mathbf{w}}} \mathrm{d}\Gamma, \qquad \forall \dot{\mathbf{P}}, \dot{\mathbf{W}}. \tag{52}$$

This requirement (referred to herein by calling the variables $\mathbf{P}$ and $\mathbf{W}$ "generalized in Prager's sense") is complied with, if matrix $\boldsymbol{\Psi}_p$ for $\tilde{\mathbf{p}}$ is derived from its counterpart for $\tilde{\mathbf{w}}$ as follows ($\mathbf{I}$ denoting identity matrix):

$$\boldsymbol{\Psi}_p(\mathbf{x}) = \boldsymbol{\Psi}_w(\mathbf{x}) \left[\boldsymbol{\Psi}_w^T \boldsymbol{\Psi}_w\right]^{-1}, \qquad \text{so that:} \qquad \int_{\Gamma_d} \boldsymbol{\Psi}_w^T(\mathbf{x}) \boldsymbol{\Psi}_p(\mathbf{x}) \mathrm{d}\Gamma = \mathbf{I}. \tag{53}$$

The orthogonality expressed by Eq. $(53)_b$, is easily seen to imply both Eq. (52) and the consequence that the generalized relative displacements $\mathbf{W}$ become weighted averages of their local counterparts, similarly to Eq. $(51)_b$ for tractions, namely:

$$\mathbf{W} = \int_{\Gamma_d} \boldsymbol{\Psi}_p(\mathbf{x}) \tilde{\mathbf{w}}(\mathbf{x}) \mathrm{d}\Gamma. \tag{54}$$

The general CCM described by Eqs. (34)–(37), involves other pairs of conjugate variables (conjugate in the sense that in each pair the dot product intervenes explicitly and/or has a mechanical meaning): $\mathbf{w}^e$, $\mathbf{p}$; $\mathbf{w}^p$, $\mathbf{p}$; $\mathbf{s}$, $\mathbf{q}$; $\dot{\boldsymbol{\lambda}}$, ϕ; $\boldsymbol{\lambda}$, $\widehat{\phi}$. In each pair, the shape functions for the former (kinematic) variable will be chosen arbitrarily, under the continuity constraint set by the "regularization" of singular integrals (Sec. 4); the shape functions for the latter (static) variable will be derived according to the pattern adopted for the conjugate pair $\mathbf{w}$, $\mathbf{p}$, Eqs. $(53)_a$.

Denoting by capital symbols the generalized counterparts of the local variables in the same lower-case letters, the relation set thus resulting from Eqs. (34)–(37) reads:

$$\mathbf{W} = \mathbf{W}^e + \mathbf{W}^p, \tag{55}$$

$$\mathbf{P} = \frac{\partial \Pi}{\partial \mathbf{W}^e}(\mathbf{W}^e, \mathbf{S}), \qquad \mathbf{Q} = \frac{\partial \Pi}{\partial \mathbf{S}}(\mathbf{W}^e, \mathbf{S}), \tag{56}$$

$$\dot{\mathbf{W}}^p = \frac{\partial \hat{\boldsymbol{\Phi}}^T}{\partial \mathbf{P}}(\mathbf{P}, \mathbf{Q})\dot{\boldsymbol{\Lambda}}, \qquad \dot{\mathbf{S}} = -\frac{\partial \hat{\boldsymbol{\Phi}}^T}{\partial \mathbf{Q}}(\mathbf{P}, \mathbf{Q})\dot{\boldsymbol{\Lambda}}, \tag{57}$$

$$\dot{\boldsymbol{\Lambda}} \geq \mathbf{0}, \qquad \boldsymbol{\Phi}(\mathbf{P}, \mathbf{Q}) \leq \mathbf{0}, \qquad \boldsymbol{\Phi}^T \dot{\boldsymbol{\Lambda}} = \mathbf{0} \tag{58}$$

having set:

$$\Pi(\mathbf{W}^e, \mathbf{S}) \equiv \int_{\Gamma_d} \pi(\tilde{\mathbf{w}}^e, \tilde{\mathbf{s}}) \mathrm{d}\Gamma = \int_{\Gamma_d} \pi(\boldsymbol{\Psi}_w \mathbf{W}, \boldsymbol{\Psi}_s \mathbf{S}) \mathrm{d}\Gamma \,. \tag{59}$$

The following remarks are intended to clarify the meaning and implications of Eqs. (55)–(58).

(a) The CCM was originally formulated (Secs. 5 and 6) locally, at any point of the process zone Γ_d^p (or of the whole Γ_d if it is meant to cover by suitable adjustments undamaged material and actual cracks). In what precedes, the local model has given rise to a CCM which represents the behaviour of the locus Γ_d in a weighted average, global sense. This global CCM is consistent with the discretization of the BIEs governing the elastic context of the structure, (Sec. 3), because it is formulated in terms of Prager's generalized variables which include those introduced in that (Galerkin) discretization.

(b) The essential features of the local CCM (while it is locally violated) are transferred to the global CCM. In fact, the convexity (or lack thereof) of the free energy π in each subspace of its argument (and, hence, the softening behaviour) implies that of Π through its very definition, Eq. (59). The convexity of $\boldsymbol{\Phi}$ (and, hence, that of the yield domain at any time) is entailed by that of $\boldsymbol{\phi}$, subject to the weak restrictions $\boldsymbol{\Psi}_\lambda(\mathbf{x}) \geq \mathbf{0}$, $\forall \mathbf{x}$, as it may be shown on the basis of its generation according to the above criteria, namely:

$$\boldsymbol{\Phi}(\mathbf{P}, \mathbf{Q}) = \int_{\Gamma_d} \boldsymbol{\Psi}_\lambda^T \boldsymbol{\phi}(\Psi_p \mathbf{P}, \Psi_q \mathbf{Q}) \mathrm{d}\Gamma \,. \tag{60}$$

Since $\widehat{\Phi} = \Phi$ clearly implies $\widehat{\boldsymbol{\Phi}} = \boldsymbol{\Phi}$, also associativity is preserved. Discussion on these and other aspects of Prager's generalized variables can be found with reference to plastic analysis by FEM in [21, 22, 44], by SGBEM in [20, 49].

(c) The approximate, global CCM, Eqs. (55)-(58) could be generated by an alternative weak enforcement of the local one, Eqs. (34)-(37)), through variational statements (see details in [11], such as, e.g., the following one apt to generate Eq. $(56)_b$:

$$\int_{\Gamma_d} \delta \mathbf{s}^T (\mathbf{q} - \frac{\partial \pi}{\partial \mathbf{s}}) \mathrm{d}\Gamma = 0, \qquad \forall\, \delta \mathbf{s} = \boldsymbol{\Psi}_s \delta \mathbf{S}, \tag{61}$$

Clearly, the above modelling procedure leading from local to global CCM applies unaltered both to non-holonomic (in rates) and to stepwise or fully holonomic models.

8. Rate Problems and Criteria for Bifurcation and Overall Stability

The formulation of the boundary value problem in rates, around a given state, is the very basis of any quasi-static analysis of dissipative (non-holonomic) solid or structure, in plasticity as well as in the present fracture mechanics context (which can be conceived as centered on softening plasticity confined to the current process zone). This formulation is given below in (discrete) terms of Prager's generalized variables, merely by combining the following two ingredients, (i) and (ii), separately resulting from what precedes.

(i) The condensed description achieved in Sec. 3 by the SGBEM for the linear background of the problem, namely Eq. (18) re-written here in rates for the current process zone Γ_d^p (the noninteracting faces of the current true crack can be regarded as part of the unconstrained boundary, and the relevant variables condensed):

$$\dot{\mathbf{P}} = \tilde{\mathbf{Z}} \dot{\mathbf{W}} + \dot{\mathbf{P}}^E. \tag{62}$$

(ii) The CCM expressed in a weak, weighted-residual fashion for the whole current Γ_d^p as discussed in Secs. 5 and 7. However, besides associativity, the frequent hypothesis of no elasticity in interfaces

(i.e. $\mathbf{W}^e \equiv \mathbf{0}$) is assumed henceforth for brevity. Thus specialized, but still covering a fairly broad category of CCMs, Eqs. (55)–(58) in rates read:

$$\dot{\mathbf{Q}} = \frac{\partial^2 \Pi}{\partial \mathbf{S} \partial \mathbf{S}^T}(\bar{\mathbf{S}})\dot{\mathbf{S}} = \mathbf{K}_s \dot{\mathbf{S}}, \tag{63}$$

$$\dot{\mathbf{W}} = \frac{\partial \Phi^T}{\partial \mathbf{P}}(\bar{\mathbf{P}}, \bar{\mathbf{Q}})\dot{\mathbf{\Lambda}}, \qquad \dot{\mathbf{S}} = -\frac{\partial \Phi^T}{\partial \mathbf{Q}}(\bar{\mathbf{P}}, \bar{\mathbf{Q}})\dot{\mathbf{\Lambda}}, \tag{64}$$

$$\dot{\mathbf{\Phi}} = \frac{\partial \Phi}{\partial \mathbf{P}^T}(\bar{\mathbf{P}}, \bar{\mathbf{Q}})\dot{\mathbf{P}} + \frac{\partial \Phi}{\partial \mathbf{Q}^T}(\bar{\mathbf{P}}, \bar{\mathbf{Q}})\dot{\mathbf{Q}}, \tag{65}$$

$$\dot{\mathbf{\Lambda}} \geq \mathbf{0}, \qquad \dot{\mathbf{\Phi}} \leq \mathbf{0}, \qquad \dot{\mathbf{\Phi}}^T \dot{\mathbf{\Lambda}} = 0. \tag{66}$$

It should be remembered that in a rate problem only the "active" yield modes (such that $\Phi_j = 0$ in the starting state) are considered: a circumstance marked in Sec. 5 by primes, omitted henceforth to simplify notation.

Now, let us substitute Eq. $(64)_a$ into (62) and this into (65), Eq. $(64)_b$ in Eq. (63) and this into Eq. (65). Thus Eq. (65) becomes:

$$\dot{\mathbf{\Phi}} = \frac{\partial \Phi}{\partial \mathbf{P}^T}(\bar{\mathbf{P}}, \bar{\mathbf{Q}})\dot{\mathbf{P}}^E - \mathbf{M}\dot{\mathbf{\Lambda}} \tag{67}$$

having set:

$$\mathbf{M}(\bar{\mathbf{P}}, \bar{\mathbf{Q}}) \equiv \frac{\partial \Phi}{\mathbf{Q}^T}\mathbf{K}_s \frac{\partial \Phi^T}{\mathbf{Q}} + \left(-\frac{\partial \Phi}{\partial \mathbf{P}^T}\tilde{\mathbf{Z}}\frac{\partial \Phi^T}{\mathbf{P}} \right). \tag{68}$$

Equations (66) and (67) together represent a very compact formulation of the rate problem in cohesive fracture analysis [50], as a counterpart of that in plasticity [44, 46, 51]. The following circumstances are worth noting.

(a) This formulation amounts to a LCP, where the linear elastic stress response $\dot{\mathbf{P}}^E$ to external action rates is the input which defines the vector of data in the linear equation (67), which relates to each other, through matrix $\mathbf{M}$, two sign-constrained orthogonal unknown vectors $\dot{\mathbf{\Lambda}}$, $\dot{\mathbf{\Phi}}$.

(b) Matrix $\mathbf{M}$, Eq. (68), is symmetric due to: its generation via SGBEM, Secs. 2 and 3; the associativity of the CCM and its translation in terms of generalized variables. The former addend in $\mathbf{M}$ is generally negative-definite or at least non positive-semidefinite : in fact, it reflects the main constitutive feature of the adopted CCM, namely its softening which is mathematically expressed by the negative definiteness or at least lack of positive semidefiniteness of matrix $\mathbf{K}_s$ (concavity of the internal variable potential Π). The latter addend in $\mathbf{M}$ reflects the constraint provided by the surrounding elastic solid and its boundary fixity to the kinematic of the fracturing process in Γ_d^c. Mathematically, this addend is positive definite, since $-\mathbf{Z}$ is so ($\mathbf{Z}$ is singular only when the process zone is such that distorsions on it may give rise to rigid body motions, e.g. when a ligament vanishes at the end of a fracture process).

(c) Bifurcation of a fracture process means herein a multiplicity of solutions to the rate problem. For instance, at a certain stage of a four-point-shear test (or a four-point-bending test or a two-notch-tensile test) the original polar (or reflective) symmetry (to within imperfections) either may be preserved, or it may be disrupted by nonsymmetric tip advancements of the two developing cracks. The experimentally observed process is what "nature chooses" for thermodynamical reasons (see e.g. [7]) among the alternative ways of fulfilling equilibrium, geometric compatibility and material model.

In fracture simulations, it may be important to recognize the onset of possible solution branching, and to compute all incremental solutions, in order to capture the actual one. To this purposes, matrix $\mathbf{M}$ is meaningful in the light of the available LCP theory. In fact, this theory directly

provides, e.g., the following statements: the rate problem, Eqs. (66) and (67), has a unique solution when matrix $\mathbf{M}$ is positive definite (in mechanical terms: when the elastic constraints represented by its latter addend prevails on the softening effect reflected by the former); it has a discrete number of solutions, if and only if all principal minors of $\mathbf{M}$ are not zero.

Let us focus now on another mechanical issue centered on the LCP rate formulation, Eqs. (66) and (67). Clearly, thresholds of overall instability are crucial aspects of fracture processes in structures and primary objectives of their analysis technique. The second-order-work criterion of stability, adopted in Sec. 5 with reference to (local) CCMs, is widely accepted as thermodinamically sound and practically useful (see e.g. [7]). For the whole fracturing structure in point, at a given state of its evolution (Γ_d^p being the current process zone) in a continuum mechanics CCM setting, the overall second-order work can be expressed by means of the following functional [50]:

$$\delta^2\mathcal{L}\ 2\delta t^{-2} = -\int\limits_{\Gamma_d^p}\int \dot{\mathbf{w}}^T(\mathbf{x})\mathbf{Z}(\mathbf{x},\boldsymbol{\xi})\dot{\mathbf{w}}(\boldsymbol{\xi})\mathrm{d}\Gamma\mathrm{d}\Gamma + \int\limits_{\Gamma_d^p} \dot{\mathbf{p}}^T(\boldsymbol{\xi})\dot{\mathbf{w}}(\boldsymbol{\xi})\mathrm{d}\Gamma + \int\limits_{\bar{\Omega}} \dot{\boldsymbol{\varepsilon}}_c^T(\boldsymbol{\xi})\mathbf{E}\dot{\boldsymbol{\varepsilon}}_c(\boldsymbol{\xi})\mathrm{d}\Omega. \tag{69}$$

The first and second addend on the r.h.s. of Eq. (69), in view of Eq. (1), are recognized as the strain energy induced by a kinematic perturbation $\dot{\mathbf{w}}$, $\mathbf{x} \in \Gamma_d^p$, in the elastic structure and in the current process zone, respectively.

The third term, $\mathbf{E}$ being the elastic tensor (in matrix formalism) of the undamaged material, has the following meaning. Let $\dot{\mathbf{u}}$ be any field of displacement rates, continuous everywhere except across $\Gamma_d^c \cup \Gamma_d^p$, causing no stress singularity at process zone tips and vanishing on Γ_u. The perturbed configuration defined by $\dot{\mathbf{u}}$ can be conceived as reached in two stages: first, by imposing distorsions $\dot{\mathbf{w}}$ which are compatible with $\dot{\mathbf{u}}$ along Γ_d^p and generate displacements $\dot{\mathbf{u}}_w$ in $\bar{\Omega}$; second, by imposing the complement $\dot{\mathbf{u}}_c = \dot{\mathbf{u}} - \dot{\mathbf{u}}_w$ to $\dot{\mathbf{u}}_w$ with respect to $\dot{\mathbf{u}}$. The domain integral in point represents the elastic strain energy induced by the thus defined displacement field $\dot{\mathbf{u}}_c$. A proof of Eq. (69) was given in [50].

Since the third integral is a positive quadratic functional of $\dot{\mathbf{u}}_c(\mathbf{x})$, $\mathbf{x} \in \bar{\Omega}$, to stability check purposes it can be ignored, i.e. only the first one of the above two stages can be considered. As a consequence, by using Eq. (46) (i.e. Eqs. (45)–(46) specialized to associative ($\widehat{\phi} = \phi$) rigid-plastic ($\mathbf{w}^e = \mathbf{0}$) CCMs), we can derive from Eq. (69) the following sufficient and necessary condition for overall stability (cf. [44] for softening plasticity):

$$\int\limits_{\Gamma_d^p} \dot{\boldsymbol{\lambda}}^T \frac{\partial \boldsymbol{\phi}}{\partial \mathbf{q}^T}\mathbf{k}_s\frac{\partial \boldsymbol{\phi}^T}{\partial \mathbf{q}}\dot{\boldsymbol{\lambda}}\mathrm{d}\Gamma - \int\limits_{\Gamma_d^p}\int \dot{\boldsymbol{\lambda}}^T \frac{\partial \boldsymbol{\phi}}{\partial \mathbf{p}^T}\mathbf{Z}(\mathbf{x},\boldsymbol{\xi})\frac{\partial \boldsymbol{\phi}^T}{\partial \mathbf{p}}\dot{\boldsymbol{\lambda}}\mathrm{d}\Gamma\mathrm{d}\Gamma \geq 0, \quad \forall \dot{\boldsymbol{\lambda}} \geq \mathbf{0}. \tag{70}$$

The discrete approximation $\tilde{\mathbf{Z}}$ of Green functions $\mathbf{Z}(\mathbf{x},\boldsymbol{\xi})$ (generated in Sec. 3 by the SGBEM) and the corresponding discretization of the CCM in Sec. 7, permit now to directly translate the stability condition (70) in generalized variables, account taken of Eq. (68):

$$\frac{1}{2}\dot{\boldsymbol{\Lambda}}^T\mathbf{M}\dot{\boldsymbol{\Lambda}} \geq \mathbf{0}, \qquad \forall \dot{\boldsymbol{\Lambda}} \geq \mathbf{0}. \tag{71}$$

The above achieved result can be elucidated by the remarks which follow.

(A) The structure is stable if and only if matrix $\mathbf{M}$ is copositive. Copositiveness defined precisely by Eq. (71), cannot be tested or established economically. Therefore, the subsequent (sufficient only, more restrictive) condition has more practical value.

(B) The structure is strictly stable if matrix $\mathbf{M}$ is positive definite. Positive definiteness of a symmetric matrix is ascertained if its least (real) eigenvalue, or a lower bound on it, is positive. This confers a practical, operative value to the above statement.

(C) Since positive definiteness of $\mathbf{M}$, which was found earlier to rule out bifurcations, is more restrictive than copositiveness which characterizes stability, it can be expected that in a CCM fracture simulation (where, as cracks propagate, the stabilizing effects of the second addend of $\mathbf{M}$ decreases) the path-branching threshold precedes the onset of instability (i.e., e.g., the peak load in

a force-controlled test). The same sequence is known to occur in elastoplastic buckling of Shanley's column, but with a continuum set of solutions, not with a discrete one like here.

(D) Conceptually and computationally notable appears now to be the role of matrix **M**. It governs important features and condenses meaningful information on the current behaviour of a CCM-idealized fracturing structure. This is subordinate to its symmetry, which the present SGBEM provides, traditional BEMs do not. The size of M is relatively small, since it may equal the number of the nodal displacement jumps in the current process zone only (unless part of the current crack Γ_d^c is included in Γ_d^p to avoid frequent changes of the matrix **A** to invert).

9. On time-stepping procedures

This section outlines some aspects of quasi-brittle fracture simulations carried out step-by-step because the crack path is not *a priori* known and/or nonholonomic CCM are required in view of local unloading (e.g. under non-proportional external actions). Since abundant sources of information are available on the general aspects of nonlinear marching solutions, only those which are peculiar of (or influenced by) the approaches adopted in this paper will be considered below.

The assumption is made for simplicity that the external actions are governed by a load factor, say $\alpha(t)$, which multiplies a reference distribution and, hence, all linear consequences of this, like, e.g. the elastic response on Γ_d or Γ_d^p, say $\bar{\mathbf{p}}^E = \Psi_p \bar{\mathbf{P}}^E$.

(A) Situations prone to the use of piecewise linear CCMs (like in Fig. 1) can be dealt with by a very simple *ad hoc* procedure, which exploits the PWL nature of the CCM and the compact rate formulation of Sec. 8. This technique can be summarized in its operational phases as follows [9]. (i) In the current known situation formulate the rate problem (66) and (67) considering only the active modes ($\Phi_j = 0$) and solve for $\dot{\alpha} = 1$ this LCP by one of the algorithms mentioned in Sec. 10. If there are more solutions, select the one with minimum second-order work $\delta^2\mathcal{L}$; if there is no solution solve for $\dot{\alpha} = -1$. (ii) Scale linearly the above solution up to activation of a new yield mode, thus determining the step amplitude $\Delta\alpha$ and, hence, the increments of all variables. (iii) Update the LCP Eqs. (66) and (67) accomodating in it the new yield mode. Further details and remarks on this can be found in [9]. Its pros are: the bifurcation and overall stability checks of Sec. 8 are integrated, not separate, parts of the evolutive analysis; no special provision is required by instabilities (normal or snap-back); no further approximations are implied by the finite amplitude of the step. The main disadvantages: steps may become very small for numerous variables; no generalization possible to non PWL models.

(B) When general (non PWL) CCM have to be employed, say in the form of Eqs. (55)–(58), the step-by-step fracture analysis becomes centered on the strategy adopted to formulate and iteratively solve the (nonlinear) finite-step problem. This strategy has much in common with elastic-plastic analysis in the presence of softening (cf. e.g. [51]) with two main differences: mesh-dependence is not expected here (CCMs interpret localization at its limit and, in a sense, represents a "regularization" provision); the search for the advancement direction of the process zone tips, to be commented upon below at (C). Since time integration schemes in plasticity and in nonlinear fracture mechanics by BEMs or FEMs are basically similar and are dealt with in an abundant literature, only a few distinctive aspects are briefly mentioned below. (a) In fracture mechanics the most natural driving variable is the tip advancement (in a pre-computed direction, usually iteratively adjusted) in the spirit of the indirect displacement control approaches stemming from Riks "arc length" method [58], so that the load factor increment $\Delta\alpha$ is an unknown and instability thresholds are easily overcome. (b) The formulation of the step-holonomic nonlinear CCM in finite increments, say $\Delta\mathbf{p} = f(\Delta\mathbf{w})$, or $\Delta\mathbf{P} = F(\Delta\mathbf{W})$, is usually implicit, e.g. according to the backward difference scheme (i.e. with unknown gradients, computed at the step-end), primarily in view of better algorithmic stability property (even if softening makes only "conditional", i.e. occurring for suitably small Δt, the contractivity of disturbance along the step-sequence). (c) Obviously, CCMs are formulated in local references, so that coordinate transformations are recurrent when, at each iteration, the nonlinear

constitutive relation $\Delta\mathbf{P} = F(\Delta\mathbf{W})$ must be combined with the linear elastic one, namely with Eqs. (18) in increments for the current Γ_d^p (or $\Gamma_d^p \cup \Gamma_d^c$) and with the tip advancement constraint. (d) The imposed tip advancement means to add BEs in the direction dictated by the adopted criterion, with possible local re-meshing and adjustments of the shape functions as mentioned in the subsequent paragraph.

(C) When the locus Γ_d of possible kinematic discontinuities is not known or conjectured *a priori*, at each step of an evolutive analysis the search for the advancement direction of the process zone tip is an important phase, particularly delicate in BEM. The frequently adopted criterion of "maximum circumferential stress" entails the computation of the stresses at the tip of the process zone for the determination of the direction θ_c which maximizes the stress $\sigma_{\theta\theta}$, θ being the angle coordinate in a local polar reference system $\{r, \theta\}$ centered on the tip.

In cohesive fracture mechanics, stresses at the tip of the process zone are finite and can thus directly be computed resorting to Somigliana integral representation for stresses σ_{ij}. This reduces to the evaluation of the displacement gradient since, through Hooke's law and compatibility: $\sigma_{ij} = E_{ijkl}(\partial/\partial x_l)u_k$. Actual displacements in any point of Γ can be conceived (like in Sec. 2) as superposed effects of sources $\mathbf{f}^* = \mathbf{p}^+ - \mathbf{p}^-$, $\hat{\mathbf{d}}^* = \mathbf{u}^+ - \mathbf{u}^-$ on Γ and $\mathbf{w}^*$ on Γ_d, provided that the exterior domain is recognized as unstressed and undeformed ($\mathbf{p}^+ = \mathbf{u}^+ = 0$) and the data and the solution of the current instant $\bar{t}$ are entered ($\mathbf{p}^- = \bar{\mathbf{p}}$ on Γ_p, $\mathbf{u}^- = \bar{\mathbf{u}}$ on Γ_u, $\mathbf{u}^- = \mathbf{u}$ on Γ_p, $\mathbf{p}^- = \mathbf{p}$ on Γ_u, $\mathbf{w}^* = \mathbf{w}$ on Γ_d). Thus the collocation displacement equation reads

$$\mathbf{u}(\boldsymbol{\xi}) = \int_\Gamma \left[\mathbf{G}_{uu}^T \mathbf{p}(\mathbf{x}) - \mathbf{G}_{pu}^T \mathbf{u}(\mathbf{x})\right] \mathrm{d}\Gamma_x + \int_{\Gamma_d} \mathbf{G}_{pu}^T \mathbf{w}(\mathbf{x}) \mathrm{d}\Gamma_x. \tag{72}$$

The displacement gradient is obtained by differentiating Eq. (72) with respect to coordinate ξ_k:

$$\frac{\partial \mathbf{u}(\boldsymbol{\xi})}{\partial \xi_k} = \int_\Gamma \left[\frac{\partial \mathbf{G}_{uu}^T}{\partial \xi_k} \mathbf{p}(\mathbf{x}) - \frac{\partial \mathbf{G}_{pu}^T}{\partial \xi_k} \mathbf{u}(\mathbf{x})\right] \mathrm{d}\Gamma_x + \int_{\Gamma_d} \frac{\partial \mathbf{G}_{pu}^T}{\partial \xi_k} \mathbf{w}(\mathbf{x}) \mathrm{d}\Gamma_x. \tag{73}$$

If Eq. (73) is collocated at the crack tip without any additional hypothesis on $\mathbf{w}$, the last hypersingular integral does not yield a finite value. This is physically correct only in linear fracture mechanics where strains are not bounded at crack tips (e.g. [25]). In cohesive fracture mechanics, on the contrary, it is well known that not only the displacement discontinuity does vanish at the crack tip, but also its tangential derivative. Let $\mathbf{w}$ be $C^{1,\alpha}$ continuous at the crack tip, i.e. $|\mathbf{w}| = O(r^{1+\alpha})$ with $0 < \alpha \leq 1$. Then $(\partial/\partial\xi_k)\mathbf{G}_{pu}\mathbf{w}$ behaves like $O(r^{\alpha-1})$ (i.e. it is only weakly singular) and can be integrated. This implies that nonconventional modelling of the $\mathbf{w}$ field has to be employed at process zone tips: e.g., cubic Hermitian shape functions or suitable combinations of quadratic Lagrangian shape functions.

10. Holonomic Analysis and Multiplicity of Solutions

In Sec. 6 some path-independent CCMs have been considered for the analysis of structures in situations where the locus of possible discontinuities Γ_d can be assumed a priori and "local unloading" in the process zone can be reasonably conjectured as negligible, in view of the monotonous and proportional history of the external loads. Typical examples of such situations are three-point-bending (3PB) tests and, often but not always [52], two-notch-tensile (2NT) tests, referred to in what follows for illustration.

As an appealing alternative to customary but expensive time-stepping (evolutive) procedures, the holonomic, single-step analysis of the structural response (including cohesive cracks) to given external actions, can be carried out in the spirit of nonlinear elasticity, but exploiting peculiar features of the fracture mechanics problems of concern here.

Let us consider first piecewise-linear (PWL) holonomic CCMs for mode I fracture, specifically the one with break point of Fig.1_b. The interest of PWL kinds of CCM rests on the following

circumstances: (a) mathematically, they lead to overall analysis formulations analogous to those for rate problems, namely to LCP; (b) computationally, they are especially apt to an investigation of the important issue of multiplicity of solutions, [12].

The possibility of a discrete number of solutions was mentioned in Sec. 8 with reference to rate problems and bifurcations (i.e. to branching of equilibrium path). Multiple solutions to holonomic analysis problems are frequently expected. E.g., in simulations of 3PB tests, for a given external force we may have no solution or two solutions. In 2NT test simulations, for assigned force below the peak load four solutions may be possible for some geometries: symmetric (with respect to the specimen axis) on the ascending branch of the tension-displacement plot; symmetric on the post-peak descending branch; unsymmetric with deflection on one side; unsymmetric on the other side, cf. [7, 12].

The analytical description, Eqs. (47) and (48), of the local PWL holonomic CCM with break-point, re-written in matrix notation with self-evident meaning of the new symbols, reads:

$$\phi = \mathbf{h}\lambda + \mathbf{c}p - \mathbf{d} \leq \mathbf{0}, \qquad \lambda \geq 0, \qquad \phi^T \lambda = 0. \tag{74}$$

It is assumed that the locus Γ_d is along a symmetry axis (say axis x) of the considered solid, so that there is no shear ($p_s = 0$; $p = p_n$), like in the 3PB and in the 2NT tests. This drastic restriction is dictated by two facts: this CCM was proposed and experimentally corroborated for mode I, while its extension to mixed modes is questionable; local-global transformation of coordinates can be ignored for brevity.

The transition from the local CCM (74) to its global, weak approximation over Γ_d, follows the pattern discussed in Sec. 7, leading to a LCP qualitatively analogous to Eq. (74), but in generalized variables (capital symbols):

$$\mathbf{\Phi} = \mathbf{H}\mathbf{\Lambda} + \mathbf{C}\mathbf{P} - \mathbf{D} \leq \mathbf{0}, \qquad \mathbf{\Lambda} \geq 0, \qquad \mathbf{\Phi}^T \mathbf{\Lambda} = 0. \tag{75}$$

The meaning of the new symbols flows from Sec. 7: e.g. considering vector $\mathbf{c}$ containing material parameters: $\mathbf{C} = \int_{\Gamma_d} \Psi_\lambda \mathbf{c} d\Gamma$. Since $\mathbf{W}$ is a subvector of $\mathbf{\Lambda}$ and can be extracted by multiplying $\mathbf{\Lambda}$ by a Boolean matrix, say $\mathbf{W} = \mathbf{B}\mathbf{\Lambda}$, the substitution in Eq. (75) of the generalized tractions $\mathbf{P}$ by the linear equation (18) generated by the SGBEM, leads to:

$$\mathbf{\Phi} = \hat{\mathbf{M}}\mathbf{\Lambda} + \mathbf{V} \leq \mathbf{0}, \quad \mathbf{\Lambda} \geq \mathbf{0}, \quad \mathbf{\Phi}^T \mathbf{\Lambda} = \mathbf{0} \tag{76}$$

having set:

$$\hat{\mathbf{M}} \equiv \mathbf{H} + \mathbf{C}\tilde{\mathbf{Z}}\mathbf{B}, \quad \mathbf{V} \equiv \mathbf{C}\mathbf{P}^E - \mathbf{D}. \tag{77}$$

This compact formulation, Refs. [9, 10], of the holonomic analysis exhibits some peculiar features: due to the PWL nature of the assumed CCM it is a LCP, precisely as the rate formulation, Eqs. (66) and (67), based on a much broader category of CCMs; matrix $\mathbf{M}$ there was symmetric, not so is $\hat{\mathbf{M}}$ here; $\hat{\mathbf{M}}$ is generally not positive definite, whereas $\mathbf{M}$ is first positive definite and then (with spreading damage) it ceases being so, thus permitting path bifurcations and overall instabilities as seen in Sec. 8. Hence multiple solutions to holonomic analyses of fracturing processes are expected both from a mathematical and a mechanical standpoint (as shown by 3PB and 2NT tests).

How to compute numerically all solutions (or prove that none exists)? This question, already formulated in Sec. 8 for rate problems, appears to be at present a challenge in this and in other contexts of nonlinear mechanics (and probably of applied mathematics as well). A partial answer is given concisely below on the basis of recent investigations [8, 9, 10, 63].

(A) For any LCP and, hence, for bifurcation problems in rates with general CCM and for holonomic analysis with PWL models, there are so-called enumerative algorithms [12, 35] which do provide all solutions through a sequence of linear programming (LP). The pros are: finite termination (i.e., like in LP, all solutions are attained exactly, to within round-off errors, after a finite number of arithmetic operations); proof that no solution exists (and, hence, computation of peak

loads) can be achieved very efficiently. The cons: the algorithm is combinatorial (governed by a binary graph) and, hence, the computing time grows exponentially with the number of variables (not so serious contra when the variables concern process zones only, i.e. for bifurcation analysis); extensions beyond the LCP area cannot be expected.

(B) Optimization algorithms are by far more versatile and generally more efficient than the above enumerative techniques. However, the solution, if any, achieved in a run (with asymptotic termination) depends on the initialization vector. Unfortunately, scanning the feasible domain in the space of variables by diverse initializations does not guarantee to produce all solutions, unless mechanical insight and engineering judgment help in some circumstances [12]. The following alternative strategies were examined so far to fracture analysis purposes, in the writers' knowledge.

(B1) It is readily seen that any LCP is equivalent to a nonconvex quadratic programming (QP) problem. E.g., the LCP one formulated by Eq. (76) is equivalent to:

$$\min_{\mathbf{\Lambda}}\{\mathbf{\Lambda}^T\mathbf{M}\mathbf{\Lambda} - \mathbf{C}\mathbf{\Lambda}\} = 0, \tag{78}$$

$$\text{subject to:} \quad \mathbf{M}\mathbf{\Lambda} - \mathbf{C} \leq 0, \quad \mathbf{\Lambda} \geq 0. \tag{79}$$

It can be easily shown that the solutions necessarily form a subset of the vertex set in the (hyper)polyhedron defined by (linear) inequalities (79). Equations (78) and (79) can be solved, not by classical (e.g. Lemke) QP algorithms, but by various algorithms for nonconvex constrained minimization, e.g. by those mentioned in (B2) and (B3) and by sequential quadratic programming SQP, which is a first-order algorithm solving a convex QP at each step.

(B2) It was proved (Robinson, 1992) that solutions of any complementarity problem, say $\mathbf{F}(\mathbf{\Lambda}) \leq 0$, $\mathbf{\Lambda} \geq \mathbf{0}$, $\mathbf{F}^T\mathbf{\Lambda} = \mathbf{0}$, are closely related to the solutions of the following (nonlinear) equation:

$$\mathbf{F}(\mathbf{\Lambda}_E) + (\mathbf{\Lambda} - \mathbf{\Lambda}_E) = \mathbf{0} \tag{80}$$

where: $\mathbf{F}$ is any mapping of the vector space $\mathbf{\Lambda}$ on itself (in particular, for LCPs like Eq. (76), the linear mapping through matrix $\mathbf{M}$); subscript E means Euclidean projection (replacement by zeros of all negative components of a vector). The Euclidean norm of the l.h.s. of Eq. (80) is a nonsmooth function of Λ, to be minimized by a recent extension (called "path search method") of the classical Newton method [10, 12, 27].

(B3) Genetic algorithms, applicable to both minimization problem generated in (B1) (constrained, smooth) or (B2) (unconstrained, nonsmooth), form a well-known fascinating class of numerical procedures of zero order (i.e. no derivatives are taken in the process). They turned out to be a practical tool for the inverse problem of parameters in CCM in [13], but not apt to capture multiplicity of solutions.

So far in this Section PWL holonomic CCMs for mode I were considered and (implicitly, by analogy) general nonholonomic CCMs in rates. Focusing now on Eqs. (49) and (50) as representative of mixed-mode holonomic CCMs (Fig. 2), it is worth noting that Eqs. (49) and (50) can be interpreted as partial derivatives with respect to opening w_n and sliding w_s relative displacement, respectively, of the following potential [66]:

$$\pi(\mathbf{w}) = \mathcal{G}_F\left[1 - \left(1 + \frac{w_n}{a_n}\right)\exp\left(-\frac{w_n}{a_n}\right)\exp\left(-\left(\frac{w_s}{a_s}\right)^2\right)\right]. \tag{81}$$

This can be interpreted as energy density on Γ_d associated to displacement jumps $\mathbf{w}$. It may be proven in general (proof omitted here for brevity) that the stable deformed configuration of a fracturing continuum idealized by a holonomic CCM model under given external actions (which are captured by the tractions $\mathbf{p}^E$ they cause on Γ_d in the undamaged, linear-elastic solid) is characterized by the minima (global and local) of the following functional:

$$\mathcal{E}(\mathbf{w}) = -\frac{1}{2}\int_{\Gamma_d} \mathbf{w}^T(\mathbf{x})\mathbf{Z}(\mathbf{x},\boldsymbol{\xi})\mathbf{w}(\boldsymbol{\xi})\mathrm{d}\Gamma + \int_{\Gamma_d} \pi(\mathbf{w})\mathrm{d}\Gamma - \int_{\Gamma_d} \mathbf{w}^T\mathbf{p}^E\mathrm{d}\Gamma\ . \tag{82}$$

Clearly, the lack of convexity arises from the second integral into which Eq. (81) has to be substituted if the CCM of Eqs. (49)–(50) is accepted. The algebraic approximation $\bar{\mathbf{Z}}$ of kernel $Z(\mathbf{x},\boldsymbol{\xi})$ by the SGBEM (Secs. 2-4) and the discretization in terms of generalized variables of functional $\mathcal{E}$ according to Sec. 7, reduce $\mathcal{E}$ to a function of $\mathbf{W}$. The unconstrained minimization of this (nonconvex, nonsmooth) function can be carried out by the general techniques mentioned in (B), i.e.: SPQ; classical conjugate gradient nonlinear programming procedures; genetic algorithms.

Obviously, other general techniques are available for nonconvex (and constrained and nonsmooth) minimization, and might be useful in the present context. According to recent computational experience (cf. [10, 12]), the path solver (cf. B2) turned out to be especially versatile and efficient in all situations, also because it was implemented in a sophisticated computer code (PATH, [27]). In closing, it is worth noting the fundamental role of the SGBEM in preserving both the essential features of the first integral in Eq. (82) and its energy meaning.

11. Closing remarks

In this paper, first a symmetric Galerkin boundary element method (SGBEM) has been briefly presented in linear elasticity, in view of its application to nonlinear quasi-brittle fracture mechanics centered on cohesive crack models (CCM). Then certain classes of such models available in the literature have been mathematically described (without discussing their origin and experimental basis). Finally, the SGBEM and CCM have been combined with some peculiar algorithms of mathematical programming (not considered here in any detail).

Some issues with mathematical and/or computational interest have been critically presented, and are believed to corroborate the potentialities of the recently developed SGBEM in fracture analysis of concrete and other quasi brittle materials and its presumable advantages, at least with respect to traditional BEMs, in fracture simulations. In this respect, it is worth noting that either "zoning", see e.g. [25], or the "dual approach", see e.g. [40], [19], are required in traditional BEMs for fracture simulations, while they are not needed in SGBEM.

Among the related topics not covered in this paper (and still subjects of current research) are: overall stability criteria with nonassociative CCM; extension to dynamic fracture, e.g. in view of the seismic vulnerability assessment of concrete dams with cracks; indirect identification of material parameters in CCM.

The last issue (inverse problems) appears to be timely and especially pertinent in the present context. A particular but representative inverse problem in this area is the identification of the four parameters in the piecewise linear CCM with breakpoint. It was shown in [13] that such parameter identification can be efficiently carried out in practice by 3PB tests, displacement measurements (via speckle techniques) and minimization of a suitable computed-measured discrepancy norm, through one of the techniques mentioned in Sec. 10 (B), based on a mathematical model combining SGBEM with the PWL holonomic CCM of Sec. 6.

Appendix A. Expressions of kernels in plane strain elasticity

$\mathbf{G}_{uu}(\mathbf{x},\boldsymbol{\xi})$: i^{th} displacement component in $\mathbf{x}$ due to the j^{th} static source component in $\boldsymbol{\xi}$, in isotropic elasticity:

$$G^{ij}_{uu}(\mathbf{x},\boldsymbol{\xi}) = -\frac{1}{16\pi(1-\nu)\mu}\left[(3-4\nu)\delta_{ij}\log r - \frac{\partial r}{\partial x_i}\frac{\partial r}{\partial x_j}\right] \tag{83}$$

where ν and μ denote the Poisson's coefficient and the shear modulus, respectively,
$\mathbf{G}_{pu}(\mathbf{x},\boldsymbol{\xi})$: i^{th} traction component in $\mathbf{x}$ due to the j^{th} static source component in $\boldsymbol{\xi}$:

$$\mathbf{G}^{ij}_{pu}(\mathbf{x},\boldsymbol{\xi}) = \frac{1}{4\pi(1-\nu)}\frac{1}{r}\left\{\left[(1-2\nu)\delta_{ij} + 2\frac{\partial r}{\partial x_i}\frac{\partial r}{\partial x_j}\right]\frac{\partial r}{\partial x_k}n_k + (1-2\nu)\left(\frac{\partial r}{\partial x_i}n_j - \frac{\partial r}{\partial x_j}n_i\right)\right\} \tag{84}$$

$\mathbf{G}_{up}(\mathbf{x},\boldsymbol{\xi})$: i^{th} displacement component in $\mathbf{x}$ due to the j^{th} kinematic source component in $\boldsymbol{\xi}$:

$$\mathbf{G}_{up}^{ij}(\mathbf{x},\boldsymbol{\xi}) = -\frac{1}{4\pi(1-\nu)}\frac{1}{r}\left\{\left[(1-2\nu)\delta_{ij}+2\frac{\partial r}{\partial x_i}\frac{\partial r}{\partial x_j}\right]\frac{\partial r}{\partial x_k}m_k-(1-2\nu)\left(\frac{\partial r}{\partial x_i}m_j-\frac{\partial r}{\partial x_j}m_i\right)\right\} \tag{85}$$

$\mathbf{G}_{pp}(\mathbf{x},\boldsymbol{\xi})$: i^{th} traction component in $\mathbf{x}$ due to the j^{th} kinematic source component in $\boldsymbol{\xi}$. As for the kernel $\mathbf{G}_{pp}$, peculiar of the SGBEM of concern here, its lengthy explicit expression can be formulated in terms of $\mathbf{G}_{up}$ as follows:

$$G_{pp}^{ij}(\mathbf{x},\boldsymbol{\xi}) = \frac{2\nu\mu}{(1+\nu)(1-2\nu)}\frac{\partial G_{up}^{kj}}{\partial x_k}n_i+\mu\left[\frac{\partial G_{up}^{ij}}{\partial x_k}+\frac{\partial G_{up}^{kj}}{\partial x_i}\right]n_k. \tag{86}$$

ACKNOWLEDGMENTS

This paper has been written while both authors were visiting the Civil Engineering Department of the University of Minnesota, Minneapolis, the senior author as MTS Visiting Professor. The friendly and stimulating environment found there and the MTS support are gratefully acknowledged. The research project on quasi-brittle fracture, which led to some of the results presented here, was funded by CNR-ST/74.

REFERENCES

[1] M.H. Aliabadi and D.P. Rooke. *Numerical Fracture Mechanics*, Kluwer Academic Press, Dordrecht, 1991.

[2] A.M. Alvaredo and R.J. Torrent. The effect of the shape of the strain-softening diagram on the bearing capacity of concrete beams, *Mat. Struct.*, **20**: 448–454, 1987.

[3] H. Antes and P.D. Panagiotopulos. *The Boundary Integral Approach to Static and Dynamic Contact Problems*, Birkhäuser, Basel, 1992.

[4] C. Balakrishna, L.J. Gray and J.H. Kane. Efficient analytical integration of symmetric Galerkin boundary integrals over curved elements: thermal conduction formulation, *Comp. Meth. Appl. Mech. Engng.*, **117**: 157–179, 1994.

[5] L. Biolzi and J.F. Labuz. Global instability and bifurcation in beams composed of rock-like materials, *Int. J. Solids Structures*, **30**: 359–370, 1993.

[6] Z.P. Bazant. Instability, ductility and size effects in strain-softening concrete, *ASCE J. of Engng. Mech.*, **102**: 331–344, 1976.

[7] Z.P. Bažant and L. Cedolin. *Stability of Structures*, Oxford University Press, New York, 1991.

[8] G. Bolzon, G. Cocchetti, G. Maier, G. Novati and G. Giuseppetti. Boundary element and finite element analysis of dams by the cohesive crack model: a comparative study. In: Bourdarot, E.J. Mazars and V. Saouma, *Dam Fracture and Damage*, Balkema, Rotterdam 69–78, 1994.

[9] G. Bolzon, G. Maier and G. Novati. Some aspects of quasi-brittle fracture analysis as a linear complementarity problem. In: Z.P. Bazănt, Z. Bittnar, M. Jirasek and J. Mazars. eds., *Fracture and Damage in Quasibrittle Structures*, E & FN Spon, London, 159–174, 1994.

[10] G. Bolzon, G. Maier and F. Tin Loi. Holonomic and nonholonomic simulations of quasi-brittle fracture: a comparative study of mathematical programming approaches. In: F.H. Wittman, ed., *Fracture Mechanics of Concrete Structures*, Aedificatio Publishers, Freiburg, 885–898, 1995.

[11] G. Bolzon and A. Corigliano. A discrete formulation for elastic solids with damaging interfaces, *Comp. Meth. Appl. Mech. Engng.*, **140**: 329–359, 1997.

[12] G. Bolzon, G. Maier and F. Tin Loi. On multiplicity of solutions in quasi-brittle fracture computations, *Computat. Mech.*, **19**: 511–516, 1997.

[13] G. Bolzon, D. Ghilotti and G. Maier. Parameter identification of the cohesive crack model, *Material Identification Using Mixed Numerical and Experimental Methods*, EUROMECH 357, 1997.

[14] M. Bonnet. Regularized direct and indirect symmetric variational BIE formulation for three dimensional elasticity, *Engng. Analysis with BoundaryElem.*, **15**: 93–102, 1995.

[15] M. Bonnet. *Equations Intégrales et Eléments de Frontiére*, CNRS Editions/Eyrolles, Paris 1995.
[16] A. Carini, M. Diligenti, P. Maranesi and M. Zanella. Analytical integrations for two-dimensional elastic analysis by the symmetric Galerkin boundary element method, *Computat. Mech.*, (to appear, 1998).
[17] A. Carpinteri. Softening and snap-back instability of cohesive solids, *Int. J. Num. Meth. Engng.*, **29**: 1521–1538, 1989.
[18] L. Cedolin, S. Dei Poli and I. Iori. Tensile behaviour of concrete, *ASCE J. of Engng. Mech.*, **113**: 431–439, 1987.
[19] Z. Cen and G. Maier. Bifurcations and instabilities in fracture of cohesive-softening structures: a boundary element analysis, *Fatigue Fract. Engng. Mater. Struct.*, **15**: 911–928, 1992.
[20] C. Comi and G. Maier. Extremum, convergence and stability properties of the finite-increment problem in elastic-plastic boundary element analysis, *Int. J. Solids Structures*, **29**: 249–270, 1992.
[21] C. Comi, G. Maier and U. Perego. Generalized variable finite element modelling and extremum theorems in stepwise holonomic elastoplasticity with internal variables, *Comp. Meth. Appl. Mech., Engng.*, **96**: 133–171, 1992.
[22] C. Comi and U. Perego. A generalized variable formulation for gradient dependent softening plasticity, *Int. J. Num. Meth. Engng.*, **39**: 3731–3755, 1996.
[23] A. Corigliano. Formulation, identification and use of interface models in the numerical analysis of composite delamination, *Int. Solids Structures*, **30**: 2779–2811, 1993.
[24] S.L. Crouch and A.M. Starfield. *Boundary Element Methods in Solid Mechanics*, George Allen and Unwin, 1983.
[25] T. Cruse. *Boundary Element Analysis in Computational Fracture Mechanics*, Kluwer Academic Publisher, London, 1988.
[26] M. Diligenti and G. Monegato. Finite part integrals: their occurrence and computation, *Rendiconti del Circolo Matematico di Palermo*, **33**: 39–61, 1993.
[27] S.P. Dirkse and M.C. Ferris. The PATH solver: a non-monotone stabilization scheme for mixed complementarity problems, *Optimization Methods & Software*, **5**: 123–156, 1995.
[28] A. Frangi and G. Novati. Symmetric BE method in two dimensional elasticity: evaluation of double integrals for curved elements, *Computat. Mech.*, **19**: 58–68, 1996.
[29] W.H. Gerstle and X. Ming. FEM modelling of fictitious crack propagation in concrete, *ASCE J. of Engng. Mech.*, **118**: 587–603, 1992.
[30] M. Guiggiani, G. Krishnasamy, T.j. Rudolphi and F.J. Rizzo. A general algorithm for the numerical solution of hypersingular boundary integral equations, *J. Appl. Mech.*, **59**: 604–614, 1992.
[31] G.V. Guinea. Modelling of fracture of concrete, *Mat. Struct.*, **28**: 187–194, 1995.
[32] A. Hillerborg, M. Modeer and P.E. Petersson. Analysis of crack formation and crack growth in concrete by means of fracture mechanics and finite elements, *Cem. Concr. Research*, **6**: 773–782, 1976.
[33] S. Holzer. How to deal with hypersingular integrals in the symmetric BEM, *Comm. Num. Meth. Engng.*, **9**: 219–232, 1993.
[34] A.R. Ingraffea. Theory of crack initiation and propagation in rock. In: B. Atkinson ed., *Rock Fracture Mechanics*, Academic Press, London, chap. 3, 1987.
[35] J.J. Judice and G. Mitra. An enumerative method for the solution of linear complementarity problems, *Eur. J. Operat. Res.*, **36**: 122–128, 1988.
[36] J.H. Kane and C. Balakrishna. Symmetric Galerkin boundary formulations employing curved elements, *Int. J. Num. Meth. Engng.*, **36**: 2157–2187, 1993.
[37] J.H. Kane. *Boundary Element Analysis in Engineering Continuum Mechanics*, Prentice Hall, Englewood Cliffs, N.J., 1994.
[38] B.L. Karihaloo. *Fracture Mechanics and Structural Concrete*, Longman Scientific & Technical, Harlow, Essex, 1995.
[39] G. Krishnasamy, F.J. Rizzo and T.J. Rudolphi. Hypersingular boundary integral equations: their occurrence, interpretation, regularization and computation. In: P.K. Banerjee, et. al., *Developments in Boundary Element Methods*, Elsevier, London, 1991.
[40] V.M. Leitao. *Boundary Elements in Nonlinear Fracture Mechanics*, Comp. Mech. Publ., Southampton, 1994.
[41] J. Lemaitre and J.L. Chaboche. *Mécanique des Materiaux Solides*, Dunod, Paris, 1988.
[42] H.R. Lofti and P.B. Shing. Interface model applied to fracture of masonry structures, *ASCE J. of Struct. Engng.*, **120**: 63–80, 1994.
[43] J. Lubliner. *Plasticity Theory*, Macmillan, New York, 1990.
[44] G. Maier. Incremental plastic analysis in the presence of large displacements and physical instabilizing effects. *Int. J. Solids Structures*, **7**: 345–372, 1971.
[45] G. Maier and T. Hueckel. Nonassociated and coupled flow rules of elastoplasticity for rock-like materials, *Int. J. Rock Mech. Min. Sci. & Geomech. Abstr.*, **16**: 77–92, 1979.
[46] G. Maier, A. Zavelani Rossi, and J.C. Dotreppe. Equilibrium branching due to flexural softening, *ASCE, Journal of the Structural Division*, **99**: 897–906, 1973.
[47] G. Maier and C. Polizzotto. A Galerkin approach to boundary element elastoplastic analysis, *Comp. Meth. Appl. Mech. Engng.*, **60**: 175–194, 1987.

[48] G. Maier, Z. Cen, G. Novati and R. Tagliaferri. Fracture, path bifurcations and instabilities in elastic-cohesive-softening models: a boundary element approach. In: J.G.M. Van Mier, J.G. Rots and A. Bakker. eds., *Fracture Processes in Concrete, Rock and Ceramics*, E. & FM. Spon, London, **2**: 561–570, 1991.

[49] G. Maier, S. Miccoli, G. Novati and S. Sirtori. A Galerkin symmetric boundary element method in plasticity: formulation and implementation. In: J.H. Kane, G. Maier, N. Tosaka and S.N. Atluri. eds., *Advances in Boundary Elements Techniques*, Springer Verlag, Berlin, 288–328, 1992.

[50] G. Maier, G. Novati and Z. Cen. Symmetric Galerkin boundary element method for quasi-brittle fracture and frictional contact problems, *Computat. Mech.*, **13**: 74–89, 1993.

[51] G. Maier, S. Miccoli, G. Novati and U. Perego. Symmetric Galerkin boundary element method in plasticity and gradient plasticity, *Computat. Mech.*, **17**: 115–129, 1995.

[52] G. Maier and A. Frangi. Quasi-brittle fracture mechanics by a symmetric Galerkin boundary element method, in Karihaloo, B.L., Y.W. Mai, M.I. Ripley and R.O. Ritchie., *Advances in Fracture Research*, Pergamon, Oxford, **4**: 1837–1848, 1997.

[53] G. Monegato. Numerical evaluation of hypersingular integrals, *J. Comp. Appl. Math.*, **50**: 9–31, 1994.

[54] Q.S. Nguyen. Bifurcation and instability of dissipative systems, *CISM*, 327, 1993, Springer-Verlag.

[55] N. Nishimura and S. Kobayashi. A regularized boundary integral equation method for elastodynamic crack problems, *Computat. Mech.*, **4**: 319–328, 1989.

[56] C. Polizzotto. An energy approach to the boundary element method, part I: elastic solids, *Comp. Meth. Appl. Mech. Engng.*, **69**: 167–184, 1988.

[57] C. Polizzotto. An energy approach to the boundary element method,part II: elastic-plastic solids, *Comp. Meth. Appl. Mech. Engng.*, **69**: 263–276, 1988.

[58] E. Riks. An incremental approach to the solution of snapping and buckling problems, *Int. J. Solids Structures*, **15**: 529–551, 1979.

[59] V.E. Saouma, E. Brühwiler and H.L. Boggs. A review of fracture mechanics applied to concrete dams, *Dam Engng.*, **1**: 41–57, 1990.

[60] On the numerical integration of interface elements, *Int. J. Num. Meth. Engng.*, **36**: 43–66, 1993.

[61] S. Sirtori, G. Maier, G. Novati and S. Miccoli. A Galerkin symmetric boundary element method in elasticity: formulation and implementation, *Int. J. Num Meth. Engng.*, **35**: 255–282, 1992.

[62] T. Stankowski, K. Runesson and S. Sture. Fracture and slip of interface in cementitious composites, *ASCE J. of Engng. Mech.* **119**: 292–327, 1993.

[63] F.H. Tin-Loi and X. Ferris. Holonomic analysis of quasi-brittle fracture with nonlinear softening. In: B.L. Karihaloo, Y.W. Mai, M.I. Ripley and R.O. Ritchie. eds., *Advances in Fracture Research*, Pergamon, Oxford, 1997.

[64] J.G.M. van Mier. Mode I fracture of concrete: discontinuous crack growth and crack interface grain bridging, *Cement and Concrete Resersch*, **21**: 1–15, 1991.

[65] F.H. Wittman and X. Hu. Fracture process zone in cementitious materials, *Int. Journal of Fracture*, **51**: 3–18, 1991.

[66] X. Xu and A. Needleman. Numerical simulation of fast crack growth in brittle solids, *J. Mech. Phys. Solids*, **42**: 1397–1434, 1994.